Multiple Shock Impulse Response Functions

Terri van der Zwan*

July 2023

Job market paper

[Latest version here]

Preliminary and incomplete.
Please do not distribute without permission of the author.

Abstract

This paper introduces the multiple shock impulse response function, a tool to investigate the effects of simultaneous shocks within one period. The concept generalizes individual shock impulse response functions, accounts for the dependence between shocks, and is particularly useful when contemporaneous relations are ambiguous. It is applicable to various multivariate time series models. Simulation studies underscore its necessity for accurately interpreting the total effect of simultaneous shocks and mitigating potential temporal aggregation issues, as summing individual responses can lead to over- or underestimation of the total effect. We further illustrate the relevance by assessing a monetary policy shock alongside uncertainty shocks in lower credit rating countries in the Euro area during the European debt crisis. We find that the interaction between the shocks amplify the effects compared to a monetary policy shock alone, and that multiple shock impulse response functions are necessary as simply summing individual impulse responses result in significantly different responses.

Keywords: *Generalized impulse response functions, multiple shocks, multivariate time series models, temporal aggregation*

JEL classification codes: *C32, C53*

*Erasmus School of Economics, Erasmus University Rotterdam; Tinbergen Institute. E-mail: t.vanderzwan@ese.eur.nl. I would like to thank Michel van der Wel and Erik Kole for our valuable discussions and comments, as well as the participants of the 12th ECB Conference on Forecasting Techniques for their input. I am grateful for the *Fulbright Promovendus Grant* and the *Erasmus Trustfonds' STOER fonds* for funding my research visit to University of California San Diego, and to Allan Timmermann for hosting. All errors are my own.

1 Introduction

Impulse response analysis is a widely employed tool to examine the dynamic responses of multivariate systems to unexpected shocks or disturbances.[1] Impulse response functions (IRFs) provide insights into the transmission mechanisms and feedback effects within the system. While traditional impulse response analysis as in Sims (1980b) require assumptions on the contemporaneous relations between variables in the system, often motivated by economic theory, these might be too restrictive when structural identification of the underlying causal relations between variables are ambiguous. The generalized impulse response approach of Koop et al. (1996) and Pesaran and Shin (1998) does not rely on identification of shocks according to some canonical system or economic theory, but relies on the dependence between the model shocks. While most empirical applications primarily focus on the effect of individual shocks, it is important to note that in times of crisis, economic and financial variables seem to be increasingly connected (Billio et al., 2012; Hubrich and Tetlow, 2015), making it more likely that multiple shocks can occur within a short period of time. However, the measurement frequency of the data might not be high enough to capture these dynamics. Data at a lower frequency can obscure the causal information because multiple shocks happening at a higher frequency may be aggregated within one period of the lower frequency data. Temporal aggregation could delude our understanding of the true dynamics and the interplay of shocks. Therefore, it is crucial to account for these simultaneous shocks that we observe within one period of the measurement frequency.

This paper introduces multiple shock impulse response functions, a method which enables investigation of the total effect of simultaneous shocks taking place within the same period of time. This multiple shock impulse response functions take into account the dependence between the shocks. This allows us to examine the cumulative and interactive impacts of multiple simultaneous shocks on a system. This concept is general, as it pertains to a wide variety of multivariate time series models, and it is a generalization of the individual shock generalized impulse response functions. It is particularly useful when causal relations between variables are ambiguous, and to overcome timing issues of such shocks.

To illustrate the properties and applicability of multiple shock impulse response functions, we consider a first order vector autoregression. We derive the closed form solutions of the traditional, generalized and multiple shock impulse response functions, and discuss their relation to each other. Using a set of data generating processes, we show that the multiple shock impulse response functions

[1] Impulse response analysis was popularized by Sims (1972, 1980a,b), who linked the dynamic stochastic general equilibrium models to vector autoregression models and their shocks. See Fernández-Villaverde et al. (2007) and Giacomini (2013) for details on the mapping of these structural macroeconomic models to the VAR specification.

are necessary to accurately analyze the total effect of shocks occurring simultaneously. Summing the individual impulse responses alone can lead to significant over- or underestimation, as the extent of this discrepancy relies on the correlation between the shocks. In a mixed-frequency setting based on Ghysels (2016), we show the usefulness of multiple shock impulse response functions in addressing potential temporal aggregation issues in case of multiple shocks occurring within the same lower frequency period. The multiple shock impulse response functions closely approximate the true underlying dynamics, especially compared to summing the individual responses, showing the potential in providing a more accurate representation of the combined effects of multiple shocks.

We show the practical relevance of our multiple shock impulse response functions by studying the effect of a monetary policy shock and uncertainty shocks occurring simultaneously within a one month time frame. A monetary policy shock can induce a shock in financial uncertainty, altering the perception of systematic risk. During the European debt crisis, the European Central Bank's (ECB) decision to raise interest rates amplified financial uncertainty in vulnerable EMU countries. These changes typically occur within a month, underscoring the need for a framework that can analyze the impact of multiple shocks happening within one period. Using a global vector autoregression framework (Pesaran et al., 2004), we study the effect of a monetary policy shock simultaneously with uncertainty shock in lower credit rating countries in the Euro area. This framework allows for modeling direct effects of Euro area, and country-specific shocks and for cross-country interactions.

Using multiple shock impulse response functions is particularly beneficial in this context, as it helps to overcome temporal aggregation issues and it does not require assumptions on the ordering of variables. The latter can be problematic as the contemporaneous relation between monetary policy and uncertainty remains ambiguous (see, e.g., Jurado et al., 2015), and the ordering of countries in the framework is unclear (Dees et al., 2007).

We focus on France, Germany, Italy and Spain. We use the exogenous measure of Jarociński and Karadi (2020) as a proxy for a monetary policy shock, and country-specific stress indices as a proxy for uncertainty. The model parameters are estimated using a Bayesian estimation procedure, which we also use to construct confidence bounds.

For all IRF concepts, we find responses consistent with economic theory. The interaction between a monetary policy shock and uncertainty shocks in Italy and Spain amplify the effects compared to a monetary policy shock alone. In particular, the negative effect on real GDP. Importantly, uncertainty shocks from Southern European countries can affect other countries in the Euro area, emphasizing the importance of clear communication from the ECB to mitigate such uncertainty. Next to that, the magnitudes of the multiple shock impulse response functions are larger compared to simply summing the traditional impulse responses, whereas they are smaller compared to (incorrectly) summing the generalized impulse responses. The main take-away is that the multiple shock impulse response functions are necessary to accurately analyze the combined effect, given the substantial difference compared to the summed traditional and general IRFs, as these summed responses often lie outside the confidence bounds of the multiple shock impulse response functions.

The remainder of this paper is structured as follows. In Section 2 we introduce the general formulation of impulse response analysis, and introduce our multiple shock impulse response concept. Section 3 illustrates the properties of our concept using a first order vector autoregression model, and presents simulation studies. Section 4 presents the empirical application and Section 5 concludes.

2 Framework

Impulse response function (IRF) analysis allows the researcher to investigate the dynamic interactions, propagation, and persistence of shocks within a multivariate system of variables. We start by defining a general model to illustrate the impulse response concepts. Let $\boldsymbol{y}_t$ denote a vector containing n endogenous variables, modeled by the following general multivariate time series model

$$\boldsymbol{y}_t = f(\boldsymbol{y}_{t-1}, ..., \boldsymbol{y}_{t-p}, \boldsymbol{z}_t, ..., \boldsymbol{z}_{t-q}; \boldsymbol{\theta}_{1,t}) + g(\boldsymbol{u}_t; \boldsymbol{\theta}_{2,t}), \tag{1}$$

where $f(\cdot\,; \boldsymbol{\theta}_{1,t})$ denotes a specific functional form with predetermined, possibly time-varying, parameters $\boldsymbol{\theta}_{1,t}$ of the historical values of $\boldsymbol{y}_t$ up until lag p, and deterministic and/or exogenous variables $\boldsymbol{z}_t$ and its historical lagged values up until lag q. The function $g(\cdot\,; \boldsymbol{\theta}_{2,t})$ with predetermined parameters $\boldsymbol{\theta}_{2,t}$ captures the dependencies between the n shocks $\boldsymbol{u}_t$. The shocks have mean zero and finite variances. This general form allows for specifications like linear and non-linear vector autoregression (VAR) models—with or without exogenous variables, dynamic factor models, non-linear factor models, and regime switching models such as Markov-Switching, smooth transition, and stochastic volatility models. Additionally, it allows for, for example, copula specifications on the error terms and GARCH specifications.

We first start by paraphrasing the traditional impulse response analysis framework and the generalized impulse response functions of Koop et al. (1996). We then introduce the multiple shock impulse response functions.

2.1 Traditional Impulse Response Functions

Sims (1980b) introduced the VAR, where both $f(\cdot)$ and $g(\cdot)$ of Equation (1) follow a linear specification. Specifically, the model shocks $\boldsymbol{u}_t$ are decomposed as $\boldsymbol{u}_t = \boldsymbol{C}\boldsymbol{\varepsilon}_t$, where $\boldsymbol{C}$ denotes an $n \times n$ matrix capturing the contemporaneous relations between the structural shocks $\boldsymbol{\varepsilon}_t$. Sims (1980b) linked the structural shocks of this multivariate system to macroeconomic shocks, enabling the analysis of the effect of random impulses on a dynamic system. Ever since, impulse response functions are widely used to investigate the dynamic relationships between variables in a (linear) system. We refer to the standard impulse response analysis in linear specifications as traditional impulse response functions. Traditional IRFs can be used as a tool to answer the following question: *"What is the effect of a shock of size δ at time t on variables $\boldsymbol{y}_{t+h}$ at time $t+h$, given that no other shocks hit the system from time t until $t+h$?"*. In this paper, traditional impulse response functions refer to the following definition.

Definition 1 (**Traditional impulse response functions**). *Let $\boldsymbol{y}_t$ follow a process in accordance with Equation* (1). *The traditional impulse response functions of $\boldsymbol{y}_{t+h}$ to the s-th structural shock $\varepsilon_{s,t}$ of size δ_s are defined as*

$$\begin{aligned}\boldsymbol{\Psi}^t(h, \varepsilon_t = \delta_s, \boldsymbol{\omega}_{t-1}) = &\mathbb{E}[\boldsymbol{y}_{t+h} \mid \varepsilon_{s,t} = \delta_s, u_{j,t} = 0 \, \forall j \neq s, \boldsymbol{\varepsilon}_{t+1} = ... = \boldsymbol{\varepsilon}_{t+h} = \boldsymbol{0}, \boldsymbol{\omega}_{t-1}] \\ &- \mathbb{E}[\boldsymbol{y}_{t+h} \mid \boldsymbol{\varepsilon}_t = \boldsymbol{\varepsilon}_{t+1} = ... = \boldsymbol{\varepsilon}_{t+h} = \boldsymbol{0}, \boldsymbol{\omega}_{t-1}],\end{aligned} \tag{2}$$

for horizon $h = 0, 1, ..., H$, where $\varepsilon_{s,t}$ denotes the s-th element of the disturbances $\boldsymbol{\varepsilon}_t$, and $\boldsymbol{\omega}_{t-1}$ denotes an historical path realization of the stochastic process that generates $\boldsymbol{y}_{t+h}$.

Thus, the traditional IRFs of $\boldsymbol{y}_{t+h}$ to the s-th shock $\varepsilon_{s,t}$ of size δ_s are the difference between two conditional expectations. The first conditional expectation measures the realization of $\boldsymbol{y}_{t+h}$ over time when the system is hit by a shock at time t, i.e., the perturbed realization. The second conditional expectation, often referred to as the benchmark, measures the realization of $\boldsymbol{y}_{t+h}$ when such a shock is absent.

As Koop et al. (1996) point out, the traditional IRF specification has certain properties that could be restrictive. The specification in Equation (2) implies that no other shocks take place at time t, and that there are no other shocks occurring from $t+1$ until $t+h$. Next to that, this specification conditions on a particular historical path of $\boldsymbol{y}_{t+h}$, denoted as $\boldsymbol{\omega}_{t-1}$. In order to be empirically useful, both the perturbed and benchmark realization need to be history independent, meaning that the historical path of the realization needs to be identical up until time $t-1$.

In case of multivariate systems one must impose restrictions on the structural relations between shocks in order to isolate the effect of a specific shock $\varepsilon_{s,t}$ on the system. In other words, the contemporaneous relations between the structural shocks captured by $\boldsymbol{C}$, must be specified. In practice, one imposes restrictions on $\boldsymbol{C}$ to identify the structural relations between the shocks.[2] The traditional impulse response functions are therefore also referred to as orthogonalized impulse response functions.

2.2 Generalized Impulse Response Functions

The specification of the traditional impulse response functions as in Definition 1 can be too restrictive in particular settings, such as non-linear or ambiguous underlying relations. Therefore, Koop et al. (1996) and Pesaran and Shin (1998) introduce the generalized impulse response function (GIRF) to treat these issues. The GIRF treats the impulse responses as a random variable itself in terms of historical paths and shocks. That is, the GIRF does not condition on a particular historical path and particular shock as in Equation (2), but rather on all possible histories and all possible shocks, or subsets of them. The generalized impulse response functions are defined as

$$\boldsymbol{\Psi}^G(h,\mathcal{U}_t,\mathcal{I}_{t-1}) = \mathbb{E}[\boldsymbol{y}_{t+h} \mid \mathcal{U}_t,\mathcal{I}_{t-1}] - \mathbb{E}[\boldsymbol{y}_{t+h} \mid \mathcal{I}_{t-1}], \tag{3}$$

where both the former and latter conditional expectations are random variables. Here, $\mathcal{U}_t$ denotes a set of shocks and $\mathcal{I}_{t-1}$ the non-decreasing information set available at time $t-1$. The problem of the effect of possible future shocks occurring from $t+1$ until $t+h$ is dealt with by averaging them out, i.e., by taking the expectation over these future shocks. In this paper, we refer to the generalized impulse response function as a specific one shock version of Equation (3) as defined in the following definition.

Definition 2 (**Generalized Impulse Response Functions**). *Let $\boldsymbol{y}_t$ follow a process in accordance with Equation* (1)*. The generalized impulse response equivalent of the traditional impulse response functions $\boldsymbol{\Psi}^t(h, \varepsilon_{s,t} = \delta_s, \boldsymbol{\omega}_{t-1})$ defined in Definition 1 is a specification of Equation* (3)*, where we treat the history as random, and condition on the s-th shock of size δ_s. The one shock generalized impulse response functions of $\boldsymbol{y}_{t+h}$ to the s-th shock $u_{s,t}$ of size δ_s are defined as*

$$\boldsymbol{\Psi}^g(h, u_{s,t} = \delta_s, \mathcal{I}_{t-1}) = \mathbb{E}[\boldsymbol{y}_{t+h} \mid u_{s,t} = \delta_s, \mathcal{I}_{t-1}] - \mathbb{E}[\boldsymbol{y}_{t+h} \mid \mathcal{I}_{t-1}], \tag{4}$$

for horizon $h = 0, 1, ..., H$, where $u_{s,t}$ denotes the s-th element of the disturbances $\boldsymbol{u}_t$, and $\mathcal{I}_{t-1}$ denotes the non-decreasing information set available at $t-1$.

Note that the benchmark is the same as in Equation (3), but that the first expectation is now conditioned on a fixed value for shock s at time t. The main difference in this specification compared

[2] Examples of these restrictions are zero contemporaneous restrictions (Sims, 1980b; Christiano et al., 1999), zero long-run restrictions (Blanchard and Quah, 1989; Gali, 1999), and sign restrictions (Uhlig, 2005).

to the traditional IRF is that we do neither condition on other contemporaneous shocks nor assume future shocks to be zero, but rather integrate out these effects.

The GIRF defined in Equation (4) does not require explicit restrictions on the contemporaneous relations between the shocks. Instead, the generalized impulse response captures the effect of a system-wide shock, making it an attractive solution in case the causal relation between variables is ambiguous or when shocks are endogenous.

2.3 Multiple Shock Impulse Response Functions

The generalized impulse response functions to one particular shock is given in Equation (4). However, in case of multiple shocks within a single period, possibly triggering one another, we need an alternative concept. The multiple shock impulse response function concept we introduce allows for analyzing the effect of m shocks from a set of variables occurring at time t, without making any assumptions on the underlying relation between these variables. We therefore introduce the concept of multiple shock impulse response functions, which is defined as follows.

Definition 3 (**Multiple shock impulse response functions**). *Let $\boldsymbol{y}_t$ follow a process in accordance with Equation* (1)*. Let $\mathcal{S}$ be a set of indices corresponding to the locations of $m \leq n$ shocks of interest. The multiple shock impulse response is a specification of Equation* (3)*, where we treat the history as random, and condition on the set of m shocks of corresponding impulse sizes $\boldsymbol{\delta}_{\mathcal{S}}$. The multiple shock impulse response functions of $\boldsymbol{y}_{t+h}$ to a set of shocks $\boldsymbol{u}_{\mathcal{S},t}$ of size $\boldsymbol{\delta}_{\mathcal{S}}$ are defined as*

$$\boldsymbol{\Psi}^{\mathcal{S}}(h, \boldsymbol{u}_{\mathcal{S},t} = \boldsymbol{\delta}_{\mathcal{S}}, \mathcal{I}_{t-1}) = \mathbb{E}[\boldsymbol{y}_{t+h} \mid \boldsymbol{u}_{\mathcal{S},t} = \boldsymbol{\delta}_{\mathcal{S}}, \mathcal{I}_{t-1}] - \mathbb{E}[\boldsymbol{y}_{t+h} \mid \mathcal{I}_{t-1}], \tag{5}$$

for horizon $h = 0, 1, ..., H$, where $\boldsymbol{u}_{\mathcal{S},t}$ denotes the subset the disturbances $\boldsymbol{u}_t$, and $\mathcal{I}_{t-1}$ denotes the non-decreasing information set available at $t-1$.

In this definition, the impulse response shock size $\boldsymbol{\delta}_{\mathcal{S}}$ denotes an $m \times 1$ vector rather than a scalar δ_s in Definition 2. This definition allows for impulse response analysis of a set of shocks occur in the same period, without imposing restrictions on the structural relation between these shocks, and between the remaining shocks. It is a generalization of Definition 2 in terms of shocks of interest. In other words, when we consider $m = 1$ and select the s-th shock as the shock of interest, by setting $\mathcal{S} = \{s\}$, Definition 3 is equivalent to Definition 2.

Another property of the multiple shock impulse response function is that it takes into account the dependence between the shocks and corrects for this dependence while calculating the total effect of these shocks. Therefore, in case the m shocks of interest are all independent of each other, it holds that $\boldsymbol{\Psi}^{\mathcal{S}}(h, \boldsymbol{u}_{\mathcal{S},t} = \boldsymbol{\delta}_{\mathcal{S}}, \mathcal{I}_{t-1}) = \sum_{\ell \in \mathcal{S}} \boldsymbol{\Psi}^{g}(h, u_{\ell,t} = \delta_{\ell}, \mathcal{I}_{t-1})$. When the shocks of interest are dependent on each other, the simultaneous effect of these shocks cannot be calculated as the simple sum of their one shock GIRFs. In case of inherently independent shocks, the multiple shock impulse response functions are by definition the sum of the traditional impulse responses of the shocks of interest.

All impulse response definitions mentioned above can be calculated using numerical methods. In the following section we illustrate the difference between the concepts using a simple linear vector autoregression model. This model allows for a closed-form solution of the conditional expectations and therefore an analytical solution for the impulse response functions, rather than relying on numerical simulations.

3 Illustration: A Linear Vector Autoregression Model

In order to illustrate the different concepts of impulse response functions described above, we consider a simple linear vector autoregression (VAR) process, conforming the general specification of Equation (1). Let $\boldsymbol{y}_t$ denote the n variables of interest. The VAR process with one lag is then[3]

$$\boldsymbol{y}_t = \boldsymbol{b} + \boldsymbol{B}\boldsymbol{y}_{t-1} + \boldsymbol{u}_t, \tag{6}$$

where $\boldsymbol{b}$ denotes the constant, $\boldsymbol{B}$ denotes the $n \times n$ coefficient matrix corresponding to the first lag and $\boldsymbol{u}_t$ denotes the reduced-form residuals. We make the following standard assumptions (see, e.g., Lütkepohl, 2005)

Assumption 1. *The residuals $\boldsymbol{u}_t$ of Equation* (6) *satisfy the following white noise conditions; (i)* $\mathbb{E}[\boldsymbol{u}_t] = \boldsymbol{0}$*, (ii)* $\mathbb{E}[\boldsymbol{u}_t\boldsymbol{u}_t'] = \boldsymbol{\Sigma}$*, for all t, where the covariance matrix $\boldsymbol{\Sigma}$ is positive definite and (iii)* $\mathbb{E}[\boldsymbol{u}_t\boldsymbol{u}_v'] = \mathbf{O}_n$ *for any $t \neq v$.*

Assumption 2. *The process of Equation* (6) *satisfies the stability condition. That is, all eigenvalues of $\boldsymbol{B}$ lie inside the unit circle, or equivalently,* $\det(\boldsymbol{I}_n - \boldsymbol{B}\lambda) \neq 0$ *for $|\lambda| < 1$.*

Here, $\boldsymbol{I}_n$ denotes the $n \times n$ identity matrix and $\mathbf{O}_n$ denotes the $n \times n$ zero matrix. Given that the VAR satisfies Assumption 2, there exists an infinite vector moving average (VMA) representation such that

$$\boldsymbol{y}_t = \boldsymbol{\mu} + \sum_{j=0}^{\infty} \boldsymbol{B}^j \boldsymbol{u}_{t-j}, \tag{7}$$

where $\boldsymbol{\mu} = (\boldsymbol{I}_n - \boldsymbol{B})^{-1}\boldsymbol{b}$. The VMA is expressed in terms of reduced-form residuals, i.e., $\boldsymbol{u}_t = \boldsymbol{y}_t - \mathbb{E}[\boldsymbol{y}_t|\mathcal{I}_{t-1}]$.

[3] For parsimony we consider a VAR(1) process with a constant. A VAR process with p lags can be written as a VAR(1) process using the companion form.

In order to conduct traditional impulse response analysis, one needs to define the structural relations between the shocks, i.e., orthogonalize the reduced-form residuals. That is,

$$\boldsymbol{u}_t = \boldsymbol{C}\boldsymbol{\varepsilon}_t, \tag{8}$$

such that the invertible matrix $\boldsymbol{C}$ captures the contemporaneous effects between the structural shocks $\boldsymbol{\varepsilon}_t$. For the structural shocks it holds that $\mathbb{E}[\boldsymbol{\varepsilon}_t] = \mathbf{0}$, $\mathbb{E}[\boldsymbol{\varepsilon}_t\boldsymbol{\varepsilon}_t'] = \boldsymbol{I}_n$ for all t and $\mathbb{E}[\boldsymbol{\varepsilon}_t\boldsymbol{\varepsilon}_v'] = \mathbf{O}_n$ for any $t \neq v$.

In the remainder of this section we state the traditional, one shock generalized and multiple shock impulse response functions in terms of the VAR(1) model. We then discuss the properties of these concepts, and their relation to each other. Finally, in two numerical examples, we show the necessity of using multiple shock impulse response functions for accurately assessing the total effect of simultaneously occurring shocks, as opposed to merely summing individual impulse responses. Additionally, we highlight the value of this concept in mitigating potential temporal aggregation issues.

We consider the simple case of $\boldsymbol{y}_t$ containing $n = 3$ variables, such that $\boldsymbol{\Sigma}$ is a symmetric 3×3 matrix containing (co)variances σ_{ij} between variables i and j. We consider $m = 2$ shocks of interest, where we focus on shocks in the first two variables; $\mathcal{S} \in \{1, 2\}$. As the generalized impulse response functions and multiple shock impulse response functions are order invariant, it does not matter which subset of shocks we choose to illustrate the difference between these two concepts. The traditional impulse response functions assume a specific order of the variables. In this example we assume that the first two variables can contemporaneously affect the third variable.

3.1 Traditional Impulse Response Functions

In context of a linear VAR(1) model, we follow Definition 1. Furthermore, we use the VMA representation of Equation (7) and the mapping between the reduced-form residuals and the structural shocks. Under Assumption 1–2, the traditional orthogonal impulse response functions of $\boldsymbol{y}_{t+h}$ to a structural shock $\varepsilon_{s,t}$ of size 1 are defined as

$$\begin{aligned}\boldsymbol{\Psi}^t(h, \varepsilon_{s,t} = 1, \omega_{t-1}) = \ & \mathbb{E}[\boldsymbol{y}_{t+h} \mid \varepsilon_{s,t} = 1, \varepsilon_{j,t} = 0\, \forall j \neq s, \boldsymbol{\varepsilon}_{t+1} = ... = \boldsymbol{\varepsilon}_{t+h} = \mathbf{0}, \boldsymbol{\omega}_{t-1}] \\ & - \mathbb{E}[\boldsymbol{y}_{t+h} \mid \boldsymbol{\varepsilon}_t = \boldsymbol{\varepsilon}_{t+1} = ... = \boldsymbol{\varepsilon}_{t+h} = \mathbf{0}, \boldsymbol{\omega}_{t-1}] \\ = \ & \boldsymbol{B}^h\boldsymbol{C}\boldsymbol{e}_s,\end{aligned} \tag{9}$$

for horizon $h = 0, 1, ..., H$. The selection or unit vector $\boldsymbol{e}_s$ is an $n \times 1$ vector for which all entries are 0 except entry s, which is 1. Thus, the combination $\boldsymbol{C}\boldsymbol{e}_s$ selects the s-th column of matrix $\boldsymbol{C}$. This IRF possesses the symmetry and proportionality properties in case of a linear VAR, meaning that a positive and negative shock has the same effect, and that a shock of size k is k times the effect of a shock of size 1. Next to that, the traditional IRF is history independent, as it only depends on the coefficient matrix $\boldsymbol{B}$ and contemporaneous effects matrix $\boldsymbol{C}$.

Note that the matrix $\boldsymbol{C}$ links the reduced-form residuals to the structural shocks. There are only $n(n-1)/2$ unknown parameters in the covariance matrix $\boldsymbol{\Sigma}$ of $\boldsymbol{u}_t$ due to its symmetry. However, $\boldsymbol{C}$ contains n^2 unknown parameters. The structural shocks are therefore not identified. Consequently, additional identifying restrictions need to be imposed. These restrictions are usually motivated by economic theory.

The most popular assumption is to impose zero contemporaneous restrictions or recursive identification. The variables are ordered based on their assumed causal relations, i.e., we assume that some shocks have no contemporaneous effect on specific variables in the system. In practice, the variables that are ordered first drive the dynamics of the system, and the variables that are ordered last are the slower moving variables. The contemporaneous effects matrix $\boldsymbol{C}$ can then be recovered by considering the lower triangular Cholesky decomposition of the covariance matrix $\boldsymbol{\Sigma}$, representing the recursive structure.

In our setting, we identify the contemporaneous relations by a Cholesky decomposition. We assume that variable 1 and 2 affect variable 3, but variable 3 does not affect 1 and 2 contemporaneously. In other words, variable 3 is a slow-moving variable. Therefore, summing the effect of shock 1 and 2 results in the following traditional impulse response functions

$$\sum_{s \in \mathcal{S}} \boldsymbol{\Psi}^t(h, \varepsilon_{s,t} = 1, \omega_{t-1}) = \boldsymbol{B}^h \boldsymbol{C}(\boldsymbol{e}_1 + \boldsymbol{e}_2) = \boldsymbol{B}^h \begin{bmatrix} c_{11} \\ c_{12} + c_{22} \\ c_{13} + c_{23} \end{bmatrix}, \tag{10}$$

where c_{ij} denotes the (i, j)-th element of matrix $\boldsymbol{C}$.

3.2 Generalized Impulse Response Functions

The key distinction between the traditional (orthogonalized) impulse response functions and generalized impulse response functions lies in the treatment of shocks in the VAR. While the traditional IRFs involve an orthogonal decomposition of the reduced-form shocks, GIRFs employ a conditional expectation of the correlated shock to generate a unique reduced-form solution without imposing assumptions on the structural relations. In context of one lag linear VAR model, we need to impose normality on the residuals to obtain a closed-form solution (see, e.g., Koop et al., 1996; Pesaran and Shin, 1998).

Assumption 3. *The residuals* $\boldsymbol{u}_t$ *of Equation* (6) *are identically and independently normally distributed with mean* $\mathbf{0}$ *and covariance matrix* $\boldsymbol{\Sigma}$.

We follow Definition 2 and define the one shock generalized impulse response functions of $\boldsymbol{y}_{t+h}$ to the s-th shock $u_{s,t}$ of size δ_s. Similar to the traditional IRF, we use the VMA representation of the process $\boldsymbol{y}_{t+h}$ to work out the generalized impulse response functions. Under Assumption 1–3, allowing us to use the properties of the conditional expectations of the multivariate normal distribution, we obtain

$$\begin{aligned}\boldsymbol{\Psi}^g(h, u_{s,t} = \delta_s, \mathcal{I}_{t-1}) &= \mathbb{E}[\boldsymbol{y}_{t+h} \mid u_{s,t} = \delta_s, \mathcal{I}_{t-1}] - \mathbb{E}[\boldsymbol{y}_{t+h} \mid \mathcal{I}_{t-1}] \\ &= \boldsymbol{B}^h \boldsymbol{\Sigma} \boldsymbol{e}_s (\sigma_{ss})^{-1} \delta_s, \end{aligned} \tag{11}$$

for horizon $h = 0, 1, ..., H$. Again, $\boldsymbol{e}_s$ denotes the selection vector and σ_{ss} denotes the variance of shock s, i.e., the (s, s)-th entry of the covariance matrix $\boldsymbol{\Sigma}$.

The sum of the generalized impulse responses of Equation (11) corresponding to the first shock of size δ_1 and second shock of size δ_2 at horizon h is

$$\sum_{s \in \mathcal{S}} \boldsymbol{\Psi}^g(h, u_{s,t} = \delta_s, \mathcal{I}_{t-1}) = \boldsymbol{B}^h \big(\boldsymbol{\Sigma} \boldsymbol{e}_1 (\sigma_{11})^{-1} \delta_1 + \boldsymbol{\Sigma} \boldsymbol{e}_2 (\sigma_{22})^{-1} \delta_2\big) = \boldsymbol{B}^h \begin{bmatrix} \delta_1 + \frac{\sigma_{12}}{\sigma_{22}} \delta_2 \\ \frac{\sigma_{12}}{\sigma_{11}} \delta_1 + \delta_2 \\ \frac{\sigma_{13}}{\sigma_{11}} \delta_1 + \frac{\sigma_{23}}{\sigma_{22}} \delta_2 \end{bmatrix}. \tag{12}$$

According to this concept, the response of variable 1 (the first element) depends on the size of shock 1, corrected for the the size of shock 2, depending on the correlation between both shocks. The same holds for variable 2. Therefore, this concept does not accurately represent the response of both variables to shock 1 and 2. The response of variable 3 does not depend on the correlation between the two shocks. This is a consequence of summing two single generalized impulse responses, where we condition on only one shock in each of the generalized impulse responses.

3.3 Multiple Shock Impulse Response Functions

Following Definition 3, we define the multiple shock impulse response functions for a linear VAR process. Under Assumption 1–3, we obtain a closed-form solution for the impulse response functions of m shocks at time t. The multiple shock impulse response function for m shocks is then

$$\begin{aligned}\boldsymbol{\Psi}^{\mathcal{S}}(h, \boldsymbol{u}_{\mathcal{S},t} = \boldsymbol{\delta}_{\mathcal{S}}, \mathcal{I}_{t-1}) &= \mathbb{E}[\boldsymbol{y}_{t+h} \mid \boldsymbol{u}_{\mathcal{S},t} = \boldsymbol{\delta}_{\mathcal{S}}, \mathcal{I}_{t-1}] - \mathbb{E}[\boldsymbol{y}_{t+h} \mid \mathcal{I}_{t-1}] \\ &= \boldsymbol{B}^h \boldsymbol{\Sigma} \boldsymbol{P} (\boldsymbol{P}' \boldsymbol{\Sigma} \boldsymbol{P})^{-1} \boldsymbol{\delta}_{\mathcal{S}},\end{aligned} \tag{13}$$

where $\boldsymbol{P}$ denotes an $n \times m$ permutation matrix, containing m selection vectors where the selection indices correspond to the indices $\mathcal{S}$ of interest.

The propagation of the first two shocks in this linear example depends on $\boldsymbol{B}^h$. For the multiple shock impulse response functions, we have permutation matrix $\boldsymbol{P} = [\boldsymbol{e}_1, \boldsymbol{e}_2]$ and $\boldsymbol{\delta}_{\mathcal{S}} = [\delta_1, \delta_2]'$. Using Equation (13) we obtain

$$\boldsymbol{\Psi}^{\mathcal{S}}(h, \boldsymbol{u}_{\mathcal{S},t} = \boldsymbol{\delta}_{\mathcal{S}}, \mathcal{I}_{t-1}) = \boldsymbol{B}^h \begin{bmatrix} \delta_1 \\ \delta_2 \\ \frac{\sigma_{22}\sigma_{13} - \sigma_{12}\sigma_{23}}{\sigma_{11}\sigma_{22} - \sigma_{12}^2} \delta_1 + \frac{\sigma_{11}\sigma_{23} - \sigma_{12}\sigma_{13}}{\sigma_{11}\sigma_{22} - \sigma_{12}^2} \delta_2 \end{bmatrix}. \tag{14}$$

The j-th element corresponds to the response of variable j. The multiple shock impulse response function of variable 1 and 2 isolate the shocks coming from variable 1 and 2, respectively. The response of variable 3 to shocks in both 1 and 2 depend on the correlation between the shocks and variable 3, and corrects for the correlation between shock 1 and 2.

3.4 Comparing Impulse Response Functions

The traditional, one shock generalized and multiple shock impulse response functions can be linked to each other. The traditional IRFs are responses to a one standard deviation shock in the orthogonalized shock. By setting $\delta_s = \sqrt{\sigma_{ss}}$ in the generalized impulse response functions we measure the effect of one deviation error shock. Thus, $\boldsymbol{\Psi}^g(h, u_{s,t} = \sqrt{\sigma_{ss}}, \mathcal{I}_{t-1})$ refers to the generalized impulse response functions to a one standard deviation shock. Equivalently, the multiple shock impulse responses to one standard deviation shocks in the m variables correspond to a shock size of $\boldsymbol{\delta}_{\mathcal{S}}$, containing the corresponding standard deviations to set $\mathcal{S}$. For a simultaneous shock in 1 and 2 this yields $\boldsymbol{\delta}_{\mathcal{S}} = \left[\sqrt{\sigma_{11}},\ \sqrt{\sigma_{22}}\right]'$. This is also referred to as the scaled impulse response functions.

Pesaran and Shin (1998) discuss the properties of the generalized impulse response functions in case the process $\boldsymbol{y}_t$ follows a multivariate linear model. Pesaran and Shin (1998) show that $\boldsymbol{\Psi}^t(h, \varepsilon_{s,t} = 1, \boldsymbol{\omega}_{t-1}) = \boldsymbol{\Psi}^g(h, u_{s,t} = \sqrt{\sigma_{ss}}, \mathcal{I}_{t-1})$, in case $\boldsymbol{\Sigma}$ is a diagonal matrix, i.e., when the reduced-form residuals $\boldsymbol{u}_t$ are uncorrelated. Further, in case when $\boldsymbol{\Sigma}$ is non-diagonal, the two impulse responses are the same for the first equation in the system. Let $\boldsymbol{\psi}_j^*(h, \cdot, \cdot) = \boldsymbol{e}_j' \boldsymbol{\Psi}^*(h, \cdot, \cdot)$ correspond to the j-th entry of the impulse response concept of interest. It holds that $\boldsymbol{\psi}_1^t(h, \varepsilon_{s,t} =$

$1, \boldsymbol{\omega}_{t-1}) = \boldsymbol{\psi}_1^g(h, u_{s,t} = \sqrt{\sigma_{ss}}, \mathcal{I}_{t-1})$. One could therefore calculate the generalized impulse response of a shock in variable j by ordering this variable first and calculating the traditional impulse response function using the Cholesky decomposition.

A feature of the multiple shock impulse response functions is that it takes into account the correlation between the shocks of interest. In case the shocks of interest are uncorrelated to each other, we find that the sum of generalized IRFs is equivalent to the multiple shock impulse response functions. For example, in our considered case $\mathcal{S} = \{1, 2\}$, it is easy to see that for $\sigma_{12} = 0$, Equation (12) and Equation (14) yield the same expression. Further, the sum of the scaled generalized and scaled multiple shock IRFs are equivalent to the sum of the traditional IRFs.

3.5 Numerical Examples

We consider two simulation studies to illustrate the differences between the various impulse response function concepts. In the first setting we show the need for the multiple shock impulse response functions in order to accurately analyze the total effect of multiple shocks, and in the second setting we show that the multiple shock impulse response functions can be helpful in order to overcome temporal aggregation issues.

3.5.1 Properties of the Impulse Response Concepts

The aim of this study is to shed light on the behavior of the impulse response functions in case of multiple simultaneous shocks. We consider the most simple form of Equation (6); we set the constant to zero, and consider $n = 3$ endogenous variables. The data generating process (DGP) is

$$\boldsymbol{y}_t = \boldsymbol{B}\boldsymbol{y}_{t-1} + \boldsymbol{u}_t, \qquad \boldsymbol{u}_t \sim N(\boldsymbol{0}, \boldsymbol{\Sigma}), \tag{15}$$

where

$$\boldsymbol{B} = \begin{bmatrix} 0.4 & 0.1 & 0.1 \\ 0.1 & 0.4 & 0.1 \\ 0.2 & 0.2 & 0.4 \end{bmatrix} \qquad \text{and} \qquad \boldsymbol{\Sigma} = \begin{bmatrix} \sigma_{11} & \sigma_{12} & \sigma_{13} \\ \sigma_{12} & \sigma_{22} & \sigma_{23} \\ \sigma_{13} & \sigma_{23} & \sigma_{33} \end{bmatrix}. \tag{16}$$

We examine four different parameterizations of the covariance matrix $\boldsymbol{\Sigma}$, as shown in Table 1. Recall that we focus on $m = 2$ one standard deviation shocks shocks of interest, with locations $\mathcal{S} \in \{1, 2\}$. The ordering of variables is only relevant for the traditional impulse response functions, for which we assume that both shocks can contemporaneously affect the third variable.

In order to numerically show the differences between the multiple shock impulse responses of Equation (14), summing the generalized impulse responses of Equation (12) and summing the traditional impulse responses of Equation (10). Figure 1 shows the multiple shock impulse response

Table 1: DGP parameter settings of Equation (15)

	Specification	Description
1.	$\boldsymbol{\Sigma}^{(1)} = \begin{bmatrix} 1 & 0.25 & 0.1 \\ 0.25 & 1 & 0.5 \\ 0.1 & 0.5 & 1 \end{bmatrix}$	Shock 1 and 2 covariance is positive ($\sigma_{12} > 0$), and shock covariance of 1 and 2 to 3 is positive ($\sigma_{13}, \sigma_{23} > 0$).
2.	$\boldsymbol{\Sigma}^{(2)} = \begin{bmatrix} 1 & -0.25 & 0.1 \\ -0.25 & 1 & 0.5 \\ 0.1 & 0.5 & 1 \end{bmatrix}$	Shock 1 and 2 covariance is negative ($\sigma_{12} < 0$), and shock covariance of 1 and 2 to 3 is positive ($\sigma_{13}, \sigma_{23} > 0$).
3.	$\boldsymbol{\Sigma}^{(3)} = \begin{bmatrix} 1 & 0.25 & -0.1 \\ 0.25 & 1 & 0.5 \\ -0.1 & 0.5 & 1 \end{bmatrix}$	Shock 1 and 2 covariance is positive ($\sigma_{12} > 0$), and shock covariance of 1 and 2 to 3 is negative and positive, respectively ($\sigma_{13} < 0, \sigma_{23} > 0$).
4.	$\boldsymbol{\Sigma}^{(4)} = \begin{bmatrix} 1 & 0 & 0.1 \\ 0 & 1 & 0.5 \\ 0.1 & 0.5 & 1 \end{bmatrix}$	Shock 1 and 2 covariance is zero ($\sigma_{12} = 0$), and shock covariance of 1 and 2 to 3 is positive ($\sigma_{13}, \sigma_{23} > 0$).

Note: Our illustration focuses on the effect of a simultaneous shock in variable 1 and 2 on variable 3.

functions and the generalized impulse response functions corresponding to these four specifications. In all figures, the solid dark blue star marked lines correspond to the multiple shock impulse response function of $y_{3,t}$ to shock 1 and 2, the light blue lines correspond to the individual one shock GIRF of $y_{3,t}$ to shock 1 and 2, respectively. The solid red cross marked lines are the sum of these generalized impulse response functions, and the solid yellow plus marked lines are the sum of the traditional impulse response functions. Note that for the traditional IRFs, we identify the contemporaneous relations using a Cholesky decomposition.

Figure 1 shows that the degree of over- and underestimation of the generalized impulse response functions is contingent upon the data generating process, and is therefore non-trivial to estimate a priori. In specification 1, where the covariance between the shocks of interest $\mathcal{S}$ is positive, the sum of the GIRFs and traditional IRFs overestimate the effect of both shocks, whereas for the case of negative covariance between the first and second shock (specification 2), the sum of both underestimate the total effect. The third specification, showing the case of negative and positive covariance of variable 3 to 1 and 2, is quite similar to specification 1. However, the degree of overestimation of the sum of the GIRFs at $h = 0$ is mitigated by the negative covariance between variable 1 and 3 compared to specification 1. For $h > 0$ the degree of overestimation is roughly similar to specification 1. The degree of over- and underestimation also depends on the correlation strength between the shocks of interest—when the strength increases in absolute terms, the difference between the multiple shock impulse response functions and sum of the GIRFs becomes larger. Specification 4 shows the equivalence of the sum of GIRFs, the sum of traditional IRFs and multiple shock impulse response functions described in Section 3.4 in case the shocks of interest are uncorrelated.

Figure 1: Impulse response concepts for four DGP specifications

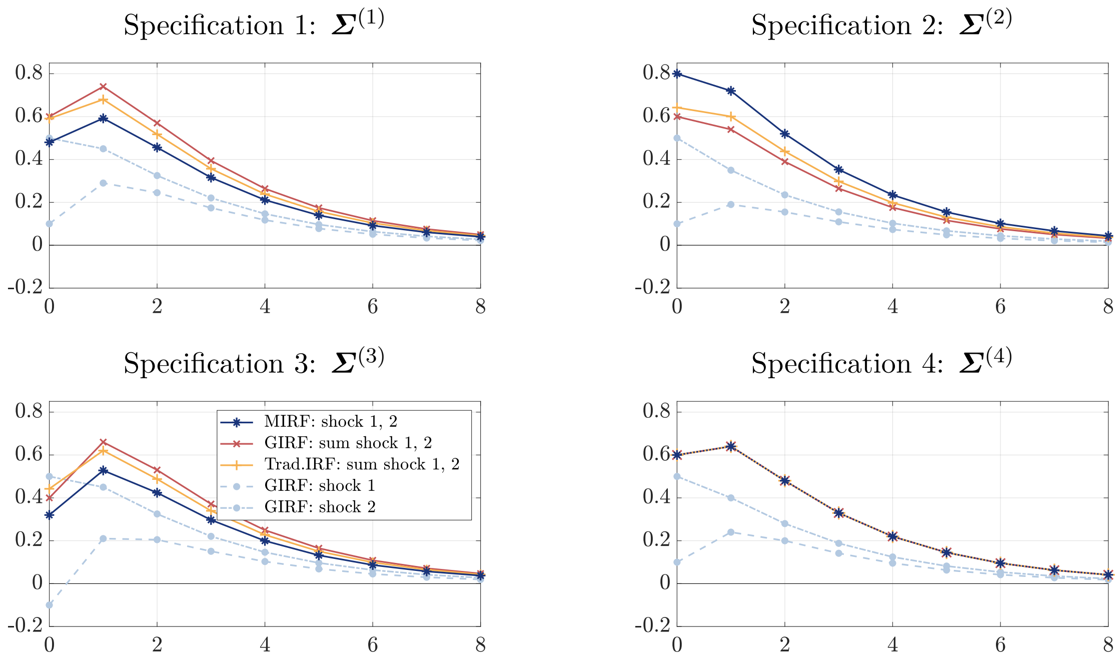

Note: The DGP specifications are given in Table 1. All impulse responses correspond to the response of variable 3 to one standard deviation shocks. The solid dark blue lines with star markers correspond to the multiple shock impulse response functions of shock 1 and 2. The solid red (cross markers) and yellow lines (plus markers) correspond to the sum of the generalized and traditional impulse response functions to shock 1 and 2, respectively. The dashed and dashed-dotted light blue lines correspond to the one shock generalized impulse response functions of shock 1 and 2, respectively.

3.5.2 Mixed Frequency and Temporal Aggregation

In the context of multiple shocks occurring, multiple shock impulse response functions can be helpful in mitigating potential temporal aggregation issues. To illustrate this, we use the framework of Ghysels (2016).[4] We consider two frequencies. Let $\{\boldsymbol{y}_t : t = 1, ..., T\}$ denote the n variables sampled at the lowest frequency. Let $\{\ddot{\boldsymbol{y}}(t, j) : t = 1, ..., T, j = 1, ..., m\}$ denote the n variables sampled m times during period t, denoting the latent multivariate high-frequency process $\ddot{\boldsymbol{y}}(t)$. As before, we consider $n = 3$ variables and set the sampling frequency at $m = 3$, reflecting a sample difference of monthly versus quarterly data. We assume that we do not observe the high frequency process. The latent higher frequency process is

$$\ddot{\boldsymbol{y}}(t) = \Big[\ddot{y}_1(t,1),\ \ddot{y}_2(t,1),\ \ddot{y}_3(t,1),\ \ddot{y}_1(t,2),\ \ddot{y}_2(t,2),\ \ddot{y}_3(t,2),\ \ddot{y}_1(t,3),\ \ddot{y}_2(t,3),\ \ddot{y}_3(t,3)\Big]'. \tag{17}$$

[4] Ghysels (2016) introduces a mixed frequency VAR framework, where high- and low frequency variables are stacked into one encompassing VAR model. This stacked skip-sampled approach is a multivariate extension of mixed-data sampling (MIDAS) regressions of Ghysels et al. (2004, 2007). In this research, we merely consider the latent stacked high frequency process and the aggregated process.

Our DGP is a VAR(1) model of the $k = n \times m$ dimensional latent process with no constant. It has a similar structure as the numerical illustration in section 6 of Ghysels (2016), where the DGP is a stacked version of a regular high frequency (monthly) VAR(1) model. The DGP has the following structure

$$\begin{bmatrix} \boldsymbol{A}_0^{1,1} & \mathbf{O}_3 & \mathbf{O}_3 \\ -\boldsymbol{A}_0^{2,1} & \boldsymbol{A}_0^{2,2} & \mathbf{O}_3 \\ \mathbf{O}_3 & -\boldsymbol{A}_0^{3,2} & \boldsymbol{A}_0^{3,3} \end{bmatrix} \ddot{\boldsymbol{y}}(t) = \begin{bmatrix} \mathbf{O}_3 & \mathbf{O}_3 & \boldsymbol{A}^{1,3} \\ \mathbf{O}_3 & \mathbf{O}_3 & \mathbf{O}_3 \\ \mathbf{O}_3 & \mathbf{O}_3 & \mathbf{O}_3 \end{bmatrix} \ddot{\boldsymbol{y}}(t-1) + \ddot{\boldsymbol{\varepsilon}}(t), \qquad \ddot{\boldsymbol{\varepsilon}}(t) \sim \mathcal{N}(\mathbf{0}, \mathbf{I}_k), \tag{18}$$

where we set

$$\boldsymbol{A}_0^{2,1} = \boldsymbol{A}_0^{3,2} = \boldsymbol{A}^{1,3} = \begin{bmatrix} 0.5 & 0.1 & 0.1 \\ 0.1 & 0.5 & 0.1 \\ 0.2 & 0.2 & 0.5 \end{bmatrix}. \tag{19}$$

The error term $\ddot{\boldsymbol{\varepsilon}}(t)$ has the same stacked structure as Equation (17). We consider four different specifications for $\boldsymbol{A}_0^{j,j}$ for $j = 1, 2, 3$, which capture the contemporaneous relations between the variables on the higher frequency. This DGP structure imposes dependency of the high frequency data on both the high- and low frequency data, and dependency of the low frequency data on both the high- and low frequency data. We set $T = 120$ quarters, a representative sample size in economic settings.

We focus on the effect of a shock in variable 1 in the first month with a shock in variable 2 taking place in the second month, on variable 3. In order to identify these shocks in the stacked latent DGP, we use the lower triangular Cholesky factorization to identify shocks as in Ghysels (2016), as it takes into account the natural order in this mixed frequency framework with the variables being ordered as in Equation (17). As a result, the identified shocks are orthogonal to each other. Therefore, the effect of the two (higher frequency) shocks is just the sum of these impulse responses, that is, $\ddot{\boldsymbol{\Psi}}^t(h, \ddot{\varepsilon}_1(t,1) = 1, \boldsymbol{\omega}_{t-1}) + \ddot{\boldsymbol{\Psi}}^t(h, \ddot{\varepsilon}_2(t,2) = 1, \boldsymbol{\omega}_{t-1})$. We sum the effect of these two shocks over the responding variables $\ddot{y}_3(t,1)$, $\ddot{y}_3(t,2)$ and $\ddot{y}_3(t,3)$ in order to obtain the total effect on the aggregated $y_{3,t}$.

Recall that the researcher does not observe the latent high frequency DGP. Instead, the researcher observes a low frequency process $\boldsymbol{y}_t = [y_{1,t},\ y_{2,t},\ y_{3,t}]'$, also referred to as the aggregated process. The aggregated process is linked to the latent process with the following aggregation scheme

$$\boldsymbol{y}_t = \begin{bmatrix} 1 & 0 & 0 & 1 & 0 & 0 & 1 & 0 & 0 \\ 0 & 1 & 0 & 0 & 1 & 0 & 0 & 1 & 0 \\ 0 & 0 & 1 & 0 & 0 & 1 & 0 & 0 & 1 \end{bmatrix} \ddot{\boldsymbol{y}}(t). \tag{20}$$

We consider the VAR(1) process of Equation (6) (without a constant) for the aggregated low frequency process $\boldsymbol{y}_t$. We estimate these reduced-form parameters with OLS.

Table 2: **DGP parameter settings of Equation (18)**

	Specification for $j = 1, 2, 3$	Description
1.	$\boldsymbol{A}_0^{j,j(1)} = \begin{bmatrix} 1 & 0 & 0 \\ 0 & 1 & 0 \\ 0 & 0 & 1 \end{bmatrix}$	No contemporaneous relation at higher frequency (within same month). Structure as in Ghysels (2016).
2.	$\boldsymbol{A}_0^{j,j(2)} = \begin{bmatrix} 1 & -0.1 & -0.1 \\ -0.1 & 1 & -0.1 \\ -0.1 & -0.1 & 1 \end{bmatrix}$	Contemporaneous relation at higher frequency between all three variables is positive.
3.	$\boldsymbol{A}_0^{j,j(3)} = \begin{bmatrix} 1 & 0.1 & -0.1 \\ 0.1 & 1 & -0.1 \\ -0.1 & -0.1 & 1 \end{bmatrix}$	Contemporaneous relation at higher frequency between variable 1 and 2 is negative, and the relation of variable 1 and 2, to 3 is positive.
4.	$\boldsymbol{A}_0^{j,j(4)} = \begin{bmatrix} 1 & -0.1 & 0.1 \\ -0.1 & 1 & -0.1 \\ 0.1 & -0.1 & 1 \end{bmatrix}$	Contemporaneous relation at higher frequency between variable 1 and 2 is positive, and the relation of variable 1 (2) to 3 is negative (positive).

Note: Our illustration focuses on the effect of a simultaneous shock in variable 1 in the first month, and variable 2 in the second month, on variable 3. Note that the off-diagonal elements of $\boldsymbol{A}_0^{j,j}$ have opposite signs, as $\boldsymbol{A}_0$ is on the left-hand side of Equation (18).

In the low frequency framework a shock in variable 1 in the first month with a shock in variable 2 in the second month corresponds to a shock in variable 1 and 2 simultaneously at time t. We calculate the sum of the traditional impulse responses to one standard deviation shocks using Equation (10), the sum of the generalized impulse responses using Equation (12), and the multiple shock impulse response functions using Equation (14), where for the generalized and multiple shock impulse responses we consider $\delta_1 = \sqrt{\sigma_{11}}$ and $\delta_2 = \sqrt{\sigma_{22}}$. We further scale the shock size of these aggregated impulse response functions by $1/\sqrt{3}$ to compare the magnitude to the magnitude of the DGP.[5]

Figure 2 shows the impulse responses for our DGP specifications. All solid lines are based on aggregated data. The solid dark lines correspond to the multiple shock IRFs, the yellow and red solid lines correspond to the traditional and generalized IRFs, respectively. The dashed dotted lines correspond to the impulse response functions originating from true underlying mixed frequency DGP. In all specifications, the traditional and generalized IRFs overestimate the true effect. The first specification shows no contemporaneous relation between the variables at the highest frequency, but a positive lagged relation between the variables at higher frequency. Specifications 2–4 show various contemporaneous correlation structures between the variables. In general, the multiple shock impulse response functions most closely resemble the true underlying DGP impulse responses—showing their potential to overcome temporal aggregation in case of multiple shocks.

[5]Note that this scaling is not completely accurate, as it relies on the assumption that the observations within the higher frequency interval are i.i.d., which is inherently not the case in our DGP specifications 2–4.

Figure 2: Impulse response concepts for four latent DGP specifications

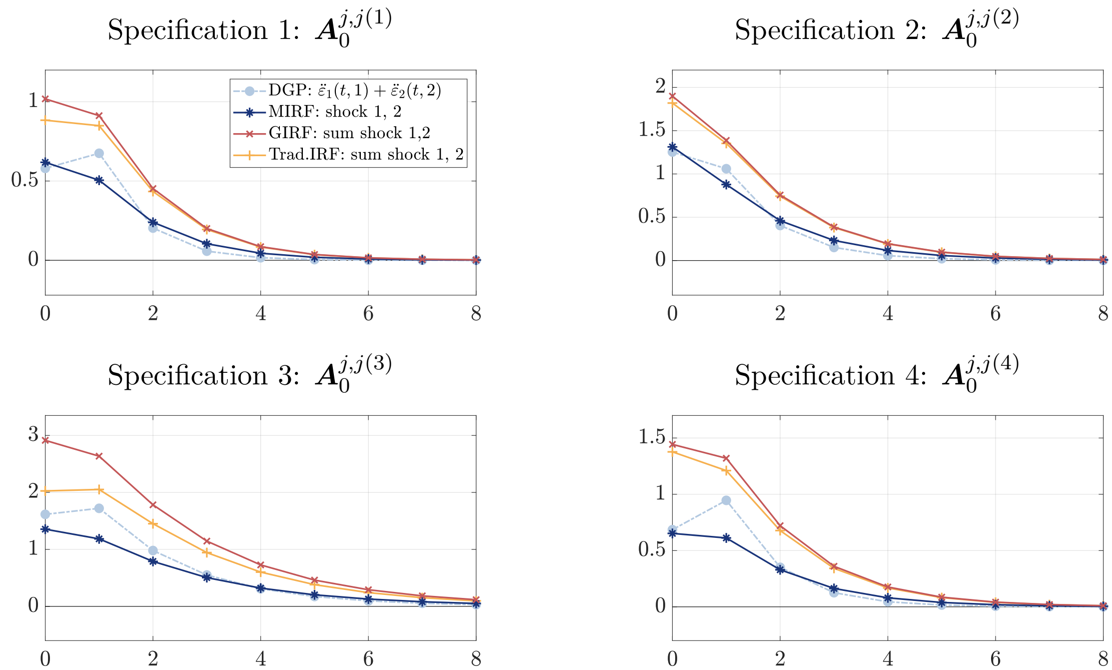

Note: The DGP specifications are given in Table 2. All impulse responses correspond to the response of variable 3 to one standard deviation shocks (in the latent process). This corresponds to a shock correction of $1/\sqrt{m}$ in the aggregated process. The x-axis corresponds to the horizon at the aggregated lower frequency. The dashed-dotted light blue line corresponds to the impulse response function to a shock in variable 1 in the first month, and a shock in variable 2 in the second month, originated from the latent (unobserved) DGP. The solid dark blue line with star markers corresponds to the multiple shock impulse response functions of shock 1 and 2. The solid red (cross markers) and yellow lines (plus markers) correspond to the sum of the generalized and traditional impulse response functions to shock 1 and 2, respectively. The sample size is $T = 120$.

4 Empirical Application: Monetary Policy and Financial Uncertainty in the Euro Area

During the European debt crisis, monetary policy tightening by the European Central Bank (ECB) to address the upward inflation path intensified financial uncertainty in already vulnerable Euro area countries such as Greece, Italy, Portugal, and Spain. See Rostagno et al. (2019) section 4.8 for an in depth discussion. This monetary tightening, combined with pre-existing vulnerabilities of the EMU, exacerbated financial uncertainty and instability (Lane, 2012). Rising borrowing costs, decline in market confidence, and interdependencies within the financial system amplified the effects,[6] leading to heightened market volatility, increased risk premiums, and risk aversion among investors.

In this application, we examine the transmission of these unanticipated changes in monetary

[6] Beirne and Fratzscher (2013) find evidence of herding behavior in sovereign yields during the debt crisis.

policy stance, referred to as monetary policy shocks, simultaneous with uncertainty shocks in lower credit rating countries. Such shocks, particularly prevalent during turbulent economic periods, abruptly alter the perceived risk of borrowers and lenders towards systematic risk in financial markets. These shocks tend to take place within a month, which is often the highest frequency available in (macro)economic settings, illustrating the need for a framework allowing to analyze the effect of multiple shocks occurring within one period and to overcome possible temporal aggregation issues. We consider four countries, France, Germany, Italy and Spain, and analyze the effect of a monetary policy shock combined with uncertainty shocks in Italy and Spain.

4.1 Global Vector Autoregression Model

We consider the global vector autoregression (GVAR) framework introduced in Pesaran et al. (2004) and extended by Dees et al. (2007), for four Euro area countries. Each country's economy is modeled by a domestic VAR, and common Euro area (monetary) factors are modeled in a separate VAR. The framework allows for modeling direct effects of Euro area and country-specific shocks, and for modeling cross-country interactions.

Let $\boldsymbol{y}_{i,t}$ be a $k_i \times 1$ vector containing variables corresponding to country i. We assume there are N countries, and for each country i there are k_i^* foreign variables $\boldsymbol{y}_{i,t}^*$ with country-specific weights and k_x common global variables $\boldsymbol{x}_t$. The domestic variables of country i follow a VARX(p_i, q_i) process

$$\boldsymbol{y}_{i,t} = \boldsymbol{c}_i + \sum_{\ell=1}^{p_i} \boldsymbol{C}_{i,\ell} \boldsymbol{y}_{i,t-\ell} + \sum_{\ell=0}^{q_i} \boldsymbol{\Lambda}_{i,\ell} \boldsymbol{y}_{i,t-\ell}^* + \sum_{\ell=0}^{q_i} \boldsymbol{\Gamma}_{i,\ell} \boldsymbol{x}_{t-\ell} + \boldsymbol{\eta}_{i,t}, \tag{21}$$

where $\boldsymbol{c}_i$ denotes the intercept, $\boldsymbol{C}_{i,\ell}$ are $k_i \times k_i$ coefficient matrices of the lagged endogenous variables, $\boldsymbol{\Lambda}_{i,\ell}$ are $k_i \times k_i^*$ coefficient matrices of the foreign-specific variables $\boldsymbol{y}_{i,t-\ell}^*$, and $\boldsymbol{\Gamma}_{i,\ell}$ are $k_i \times k_x$ coefficient matrices corresponding to the common global variables $\boldsymbol{x}_{t-\ell}$. We assume that the idiosyncratic country-specific shocks $\boldsymbol{\eta}_{it}$ are serially uncorrelated with zero mean and variance-covariance matrix $\boldsymbol{\Sigma}_{i,i}$.

The foreign-specific variables capture the relative impact of spillover effects between countries. Specifically, they are a trade-weighted sum of the variables of the other countries, such that

$$\boldsymbol{y}_{i,t}^* = \sum_{\substack{j=1 \\ j \neq i}}^{N} w_{i,j} \boldsymbol{y}_{j,t}, \quad \text{with} \quad \sum_{\substack{j=1 \\ j \neq i}}^{N} w_{i,j} = 1, \tag{22}$$

for every country i. The common global variables $\boldsymbol{x}_t$ follow a VARX(p_x, q_x) process

$$\boldsymbol{x}_t = \boldsymbol{c}_x + \sum_{\ell=1}^{p_x} \boldsymbol{\Theta}_\ell \boldsymbol{x}_{t-\ell} + \sum_{\ell=0}^{q_x} \boldsymbol{\Phi}_\ell \widetilde{\boldsymbol{y}}_{t-\ell} + \boldsymbol{\eta}_{x,t}, \tag{23}$$

where $\boldsymbol{c}_x$ is the intercept, and $\boldsymbol{\Theta}_\ell$ and $\boldsymbol{\Phi}_\ell$ are coefficient matrices. The exogenous $\widetilde{k} \times 1$ vector $\widetilde{\boldsymbol{y}}_t$ measures the Euro area economy, which is a weighted average of the domestic variables such that

$$\widetilde{\boldsymbol{y}}_t = \sum_{j=1}^{N} \widetilde{w}_j \boldsymbol{y}_{j,t}, \quad \text{with} \quad \sum_{j=1}^{N} \widetilde{w}_j = 1. \tag{24}$$

The GVAR framework allows for cross-country interactions through linkages by foreign-specific variables in Equation (21), non-zero contemporaneous dependence of shocks, e.g., $\boldsymbol{\Sigma}_{i,j} \neq 0$ for country i and j, and common Euro area factors. Exploiting that $\boldsymbol{y}^*_{i,t}$ and $\widetilde{\boldsymbol{y}}_t$ are both linear combinations of the country-specific variables $\boldsymbol{y}_{i,t}$, we can combine Equation (21) and Equation (23) into one model, such that

$$\boldsymbol{H}_0 \boldsymbol{z}_t = \boldsymbol{h}_0 + \sum_{\ell=1}^{p^*} \boldsymbol{H}_\ell \boldsymbol{z}_{t-\ell} + \boldsymbol{\varepsilon}_t, \tag{25}$$

where $p^* = \max(p, q, q_x)$, $\boldsymbol{z}_t = [\boldsymbol{x}_t', \boldsymbol{y}_t']'$, $\boldsymbol{h}_0 = [\boldsymbol{c}_x', \boldsymbol{c}']'$ and the residuals $\boldsymbol{\varepsilon}_t = [\boldsymbol{\eta}_{x,t}', \boldsymbol{\eta}_t']'$, with variance-covariance matrix $\boldsymbol{\Sigma}_e$. Provided that $\boldsymbol{H}_0$ is invertible, we obtain the reduced-form model

$$\boldsymbol{z}_t = \boldsymbol{k}_0 + \sum_{\ell=1}^{p^*} \boldsymbol{K}_\ell \boldsymbol{z}_{t-\ell} + \boldsymbol{u}_t, \tag{26}$$

where $\boldsymbol{k}_0 = \boldsymbol{H}_0^{-1} \boldsymbol{h}_0$, $\boldsymbol{K}_\ell = \boldsymbol{H}_0^{-1} \boldsymbol{H}_\ell$, and $\boldsymbol{u}_t = \boldsymbol{H}_0^{-1} \boldsymbol{\varepsilon}_t$ with $\mathbb{E}[\boldsymbol{u}_t \boldsymbol{u}_t'] = \boldsymbol{H}_0^{-1} \boldsymbol{\Sigma}_\varepsilon (\boldsymbol{H}_0^{-1})' = \boldsymbol{\Sigma}_u$. Here, $\boldsymbol{H}_0^{-1}$ captures the contemporaneous relations between the structural shocks $\boldsymbol{\varepsilon}_t$. To obtain this result, we impose the following assumptions.

Assumptions (Global VAR). *(i) The residuals $\boldsymbol{\eta}_{i,t}$ of Equation (21) and $\boldsymbol{\eta}_{x,t}$ of Equation (23) are assumed to be serially uncorrelated with zero mean and variance-covariance matrix $\boldsymbol{\Sigma}_{i,i}$ and $\boldsymbol{\Sigma}_{x,x}$, respectively. (ii) The trade-based weights $\boldsymbol{W}_i$ in Equation (22) are constant over time. (iii) Equation (26) satisfies the stability condition described in Assumption 2. (iv) The foreign-specific variables in Equation (21) are assumed to be weakly exogenous.*

The last assumption (iv) is necessary in order to estimate the model parameters in a country-per-country setting. Given the reduced-form in Equation (26), we can calculate the traditional, generalized, and multiple impulse response functions for horizon $h = 1, ..., H$ in a similar way by the following recursion

$$\boldsymbol{\Psi}^*(h,\cdot,\cdot) = \sum_{l=1}^{h} \boldsymbol{\Psi}^*(h-l,\cdot,\cdot)\boldsymbol{K}_l, \tag{27}$$

where $\boldsymbol{K}_l = 0$ in case $l > p^*$. The initial conditions are as follows: $\boldsymbol{\Psi}^t(0, \varepsilon_{s,t} = 1, \omega_{t-1}) = \boldsymbol{C}\boldsymbol{e}_s$, $\boldsymbol{\Psi}^g(0, u_{s,t} = \delta_s, \mathcal{I}_{t-1}) = \boldsymbol{\Sigma}\boldsymbol{e}_s(\sigma_{ss})^{-1}\delta_s$ and $\boldsymbol{\Psi}^{\mathcal{S}}(0, \boldsymbol{u}_{\mathcal{S},t} = \boldsymbol{\delta}_{\mathcal{S}}, \mathcal{I}_{t-1}) = \boldsymbol{\Sigma}\boldsymbol{P}(\boldsymbol{P}'\boldsymbol{\Sigma}\boldsymbol{P})^{-1}\boldsymbol{\delta}_{\mathcal{S}}$, where shock sizes δ_s and $\boldsymbol{\delta}_{\mathcal{S}}$ are set to one standard deviation shocks.

4.2 Data

We use country-specific data for France, Germany, Italy, and Spain, as these are the four largest economies in the Euro zone contributing to over 70% of the Euro zone GDP over our sample. These four countries also capture the heterogeneity within Europe in terms of solvency.[7] We consider monthly data ranging from January 1999 until October 2022.

Each domestic model includes six variables, output, prices, short- and long-term government bond yields, stock prices and a stress index capturing uncertainty. Specifically, we consider output and prices as macroeconomic indicators. We use Chow and Lin (1971) interpolation to construct a monthly proxy for economic output for each country, where we use monthly industrial production as reference series. Prices are modeled by the seasonally adjusted consumer price index (CPI). For financial variables, we use stock and bond market data. In particular, we use the 1 and 10 year government bond yields, the MSCI stock market index and the composite indicator of systematic stress (CISS), which measures the stress in financial markets for each of the four countries separately (Hollo et al., 2012). Kremer (2016) highlights the importance of including CISS indices in a macro-financial SVAR setting, as CISS contributes to the dynamics of the macroeconomy and monetary policy. The consider six foreign-specific variables, capturing the relative spill-overs between countries, which are constructed as a trade-based weighted average of all the six domestic variables. We take the natural log of output, prices and stock prices.

The common model includes the monetary policy shock series of Jarociński and Karadi (2020) as common monetary policy variable in Europe. This variable measures the exogenous interest rate surprise to a monetary policy shock coming from an announcement by the ECB.[8] The feedback variables in the common model are a GDP-weighted average of all the six domestic variables, capturing the general state of the Euro area economy as a whole.

[7]During our sample period, France's credit rating is considered high grade (AA-AAA), Germany's rating is considered prime (AAA), Italy is considered lower medium grade (about BBB) and Spain is considered medium grade (BBB-A), according to Moody's, S&P and Fitch. See `https://countryeconomy.com/ratings`.

[8]The median ECB monetary policy shock is obtained from Marek Jarociński's website. The shock is based on the price change in a 90 minute window around a ECB monetary policy event, obtained from the Euro Area Monetary Policy Event-Study Database (EA-MPD) of Altavilla et al. (2019).

4.3 Identification

We focus on the effect of a monetary policy shock, triggering financial instability in vulnerable countries, on macroeconomic and financial variables. We use an exogenous measure based on the the market responses of financial variables to an ECB monetary policy event as a proxy for a monetary policy shock, and country-specific stress indices as a proxy for uncertainty shocks. Kuttner (2001) suggests identifying monetary policy shocks through price changes in a tight window around a monetary policy announcement, as this captures the unexpected component of a monetary policy announcement (see, e.g., Gertler and Karadi, 2015; Nakamura and Steinsson, 2018). When a central bank announcement start, financial markets have already priced in the central bank's systematic response to the state of the economy. Therefore, the interest rate surprise stemming from an ECB announcement can be interpreted as a measure for the causal effect of ECB's action. We consider the median monetary policy shock of Jarociński and Karadi (2020), who distinguish between two types of shocks—action and communication—based on the correlation to the surprise in stock prices. A monetary policy shock is characterized by negative correlation between the interest rate and stock price surprise. Monetary tightening leads to higher interest rates, increasing the discount rate. Further, stock prices decrease as the expected value of future dividends also decrease. The monetary policy shock therefore isolates the component of the ECB's action.

Examples of analyzing the effects of uncertainty shocks proxied by a volatility index in a VAR framework, are Bloom (2009), Bloom (2014), Bachmann et al. (2013), Gilchrist et al. (2014), Jurado et al. (2015) and Basu and Bundick (2017). They use a Cholesky decomposition to identify these uncertainty shocks. Ludvigson et al. (2021) highlight difficulty of identifying uncertainty shocks this way, as theory is unclear about the contemporaneous relations between uncertainty and, for example, real activity. We use the country-specific CISS as a proxy for a country-specific uncertainty shock. The CISS is a stress measure based on 15 realized volatility measures from mainly the money, equity, bond, and foreign exchange markets. We focus on uncertainty shocks in Italy and Spain.

In traditional IRF analysis, the ordering is crucial for identification. The literature also remains ambiguous about the ordering. For example, Leduc and Liu (2016) and Basu and Bundick (2017) assume that monetary policy contemporaneously respond to uncertainty by ordering the federal funds rate last, whereas Gertler and Karadi (2015) and Jarociński and Karadi (2020) assume that monetary policy affects all variables in the macro-financial VARs contemporaneously. Jurado et al. (2015) consider various ordering schemes, including uncertainty as last variable, and ordering uncertainty before the federal fund rate. Next to that, in the GVAR it is unclear what the ordering of variables should be in terms of what country comes first—making traditional impulse response analysis with contemporaneous zero restrictions less attractive (see, e.g., Pesaran et al., 2004; Dees et al., 2007). By ordering the common model first in traditional IRF analysis, we assume that there is an exogenous monetary policy shock affecting all variables in the model contemporaneously. However, a shock in the systematic stress index only affects the variables ordered later than these variables. For example, when we consider the country order France, Germany, Italy, Spain, we assume that a shock in the Italian stress index only affects all the Spanish variables, including the real economic variables, contemporaneously, but this shock does not affect the French and German variables within the first month. Therefore, the anatomy of the GVAR framework makes it challenging to analyze country-specific shocks. The generalized and multiple shock impulse response functions allow for contemporaneous responses between monetary policy and uncertainty, both ways, and infer identification of these relations by using the data. They therefore remain agnostic about the ordering of shocks occurring.

4.4 Estimation

We estimate the model parameters in a country-per-country setting, as in Pesaran et al. (2004) and Burriel and Galesi (2018). We choose a parsimonious lag structure as in Burriel and Galesi (2018) based on information criteria; we set $p_i = 2$ and $q_i = 0$ for every country, such that we only consider contemporaneous relation to the exogenous variables, and we set both lags p_x, q_x to 2 for the common model.

We estimate the reduced-form parameters in a Bayesian fashion as this allows us to account for parameter uncertainty and to construct confidence bounds.[9] We use Gibbs sampling to draw from the joint posterior distribution of the reduced-form parameters, that is, we draw drawing from two conditional posterior distributions. In line with the Bayesian VAR literature, we choose a Minnesota type prior. Details on the exact procedure, prior choices and posterior distributions are reported in Appendix B. We report results based on a burn-in period of 5,000 draws, where we store every third of the following draws until we obtain 1,000 stable models from the joint posterior distribution. The Appendix reports the model diagnostics, where we show that the GVAR assumptions are adequately satisfied.

Note that by ordering the shock series first in our GVAR model, we employ the internal instrument approach, where we use the shock series as an instrument in order to identify a monetary policy shock. This method is related to the proxy VAR (Stock and Watson, 2012; Mertens and Ravn, 2013) where one identifies shocks using external instruments, where invertibility of the shock

[9] Alternative methods are applying Bayesian shrinkage to the full model (Bańbura et al., 2010), or estimating the parameters with OLS in combination with a bootstrap procedure to construct confidence bounds (e.g., Dees et al., 2007; Burriel and Galesi, 2018).

is required. Plagborg-Møller and Wolf (2021) show that ordering the instrument first, the internal instrument approach, gives valid impulse response functions even if the shock of interest is noninvertible.

4.5 Results

Figure 3 shows the impulse response functions to a one standard deviation monetary policy shock, and one standard deviation uncertainty shocks for Italy and Spain. Each row corresponds to a country. The panels illustrate the median multiple impulse response functions for monetary policy and uncertainty shocks in the two Southern European countries, shown by the dark blue line. The shaded areas indicate the 16th/84th and 5th/95th percentile ranges of the posterior distribution. The dashed blue line corresponds to both traditional and generalized impulse response functions of a monetary policy shock, due to its primary ordering in the system. The summed traditional and generalized impulse response functions are denoted by the yellow and red lines, respectively.

The responses of the variables to a monetary tightening shock are consistent with standard economic theory. Real GDP and prices decrease, whereas government bond yields slightly increase (see Jarociński and Karadi, 2020). The amplified negative effect of an uncertainty shock on the real economy is in line with amongst others Bloom (2009), Leduc and Liu (2016) and Basu and Bundick (2017), who document declining real economic activity in response to an uncertainty shock. In particular, the combined effect of a monetary policy shock and uncertainty shocks have a pronounced negative effect on real GDP and prices for all examined countries. This impact is most noticeable in Italy and Spain, although it is also apparent in France and Germany. While the immediate effects on short-term and long-term yields are minimal, a rise in these yields becomes evident over the span of one year. Further, stock prices across all countries decrease by roughly 2% within the first six months. It is worth noting that uncertainty shocks originating in Southern European nations can affect other countries in the Euro area—underlining the importance of clear and direct communication from the ECB to help avert such uncertainty.

The effect of a monetary policy shock on all variables is in general smaller in absolute terms compared to the joint effect of a monetary policy shock and uncertainty shocks. The sum of the traditional IRFs resemble the effect of the monetary policy shock, as for a lot of variables the initial response of the variables to an uncertainty shock is restricted to zero. The summed generalized IRFs overshoot the total effect. The highlight here is that for all concepts–single shock and summed versions of both traditional and generalized IRFs—the difference when compared to multiple shock impulse response functions is sizable, as they often fall outside the confidence bounds of the multiple shock IRFs, particularly within the first five months.

Figure 3: Impulse response functions to a monetary policy shock and simultaneous uncertainty shock in Italy and Spain

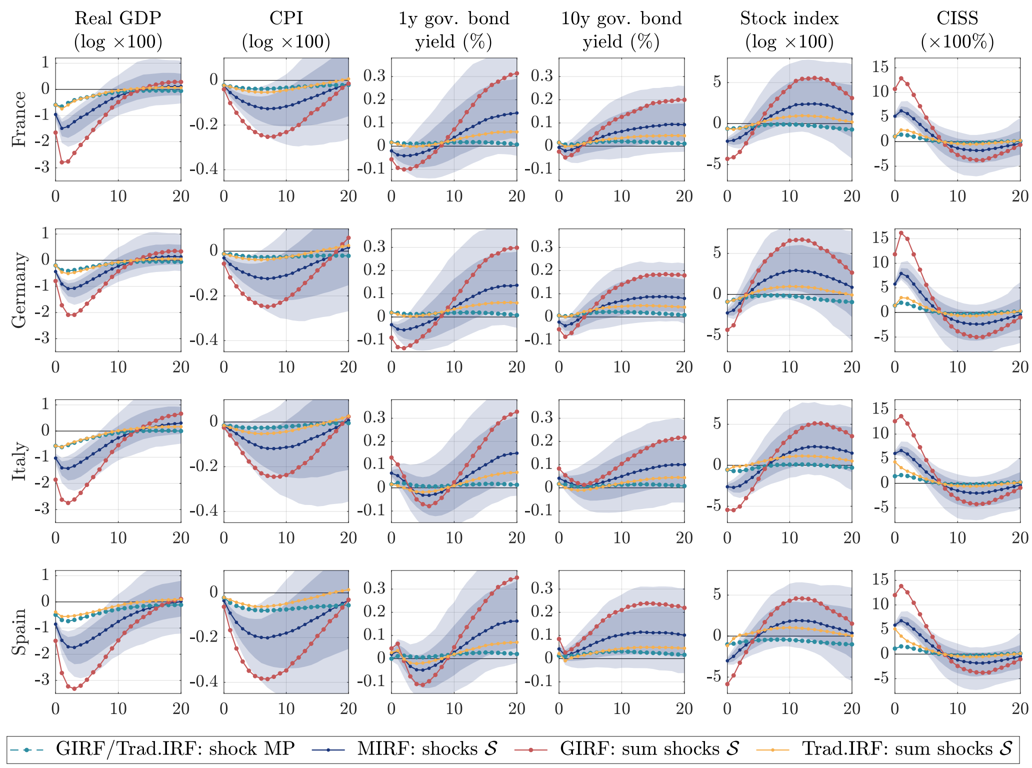

Note: All impulse responses correspond to the responses on a 20 month horizon. The solid dark blue lines correspond to the median multiple shock impulse response functions of a monetary policy shock combined with a shock in systematic risk in Italy and Spain. The darker (lighter) shaded areas correspond to 16–84th (5–95th) percentiles. The yellow lines correspond to the (coinciding) traditional and generalized median impulse responses to one monetary policy shock. The red and blue lines with correspond to the sum of the traditional and generalized median impulse response functions to all three shocks, respectively. The sample period is 01:1999-10:2022.

5 Conclusion

In this paper, we introduced multiple shock impulse response functions, which allow for the examination of the cumulative and interactive effects of multiple shocks occurring simultaneously within the same period of time. By taking into account the dependence between shocks, they provide a comprehensive framework to understand the total impact of simultaneous shocks on a system. This approach pertains to a broad set of multivariate time series models. It is particularly useful in case of ambiguous causal relations between variables, and when timing issues of shocks are challenging.

The properties of multiple shock impulse response functions are examined within the context of a first order vector autoregression model with normally distributed error terms. The closed-form solutions of traditional and general impulse response functions of Sims (1980b) and Koop et al.

(1996) are revisited, and we derive a closed-form solution for the multiple shock impulse response functions. We discuss their relation to each other, and show using simulations that multiple shock impulse response functions are necessary in order to accurately analyze the total effect of multiple shocks, as summing individual impulse responses lead to over- or underestimation depending on the correlation between the shocks. We further show in a mixed-frequency simulation setting that multiple impulse response functions are useful to address potential temporal aggregation issues, as these might arise when multiple shocks occur concurrently within a single period of the observed data frequency. The multiple shock impulse response functions tend to accurately mimic the actual underlying dynamics, providing a more precise representation of the cumulative effects of multiple simultaneous shocks, particularly when compared to just summing individual impulse responses.

We show the practical relevance of our multiple shock impulse response functions by studying the effect of a monetary policy shock and uncertainty shocks occurring simultaneously in a global vector autoregression framework of Pesaran et al. (2004). For example, during the European debt crisis, the ECB's raising interest rates amplified financial uncertainty in vulnerable EMU countries. These changes typically occur within a one month time frame. Multiple shock impulse response functions are particularly useful here, as it helps to overcome temporal aggregation issues and it does not require assumptions on the ordering of variables in the framework. We document responses consistent with economic theory for all impulse response concepts. The interaction between a monetary policy shock and uncertainty shocks in low credit rating countries amplify the effects in all EMU countries, in particular on real GDP, compared to a monetary policy shock alone, emphasizing the importance of clear communication from the ECB to mitigate uncertainty. Further, multiple shock impulse response functions provide a more accurate analysis of combined effects than just summing traditional or generalized responses, as the latter results in responses often falling outside the confidence bounds of the multiple shock impulse response functions.

In conclusion, this study makes contribution to the impulse response analysis by introducing multiple shock impulse response functions, providing a practical and effective tool to navigate the challenges associated with simultaneous shocks in multivariate models. It provides an alternative way of looking at the complex interconnected nature of economic and financial systems. For further research, it would be interesting to look at non-linear dynamics, such as second order dynamics through the lens of multiple shock impulse response functions.

References

Altavilla, C., L. Brugnolini, R. S. Gürkaynak, R. Motto, and G. Ragusa (2019). Measuring euro area monetary policy. *Journal of Monetary Economics 108*, 162–179.

Bachmann, R., S. Elstner, and E. R. Sims (2013). Uncertainty and economic activity: Evidence from business survey data. *American Economic Journal: Macroeconomics 5*(2), 217–249.

Bańbura, M., D. Giannone, and L. Reichlin (2010). Large bayesian vector auto regressions. *Journal of Applied Econometrics 25*(1), 71–92.

Basu, S. and B. Bundick (2017). Uncertainty shocks in a model of effective demand. *Econometrica 85*(3), 937–958.

Beirne, J. and M. Fratzscher (2013). The pricing of sovereign risk and contagion during the european sovereign debt crisis. *Journal of International Money and Finance 34*, 60–82.

Billio, M., M. Getmansky, A. W. Lo, and L. Pelizzon (2012). Econometric measures of connectedness and systemic risk in the finance and insurance sectors. *Journal of Financial Economics 104*(3), 535–559.

Blanchard, O. J. and D. Quah (1989). The dynamic effects of aggregate demand and supply disturbances. *American Economic Review 79*(4), 655–673.

Bloom, N. (2009). The impact of uncertainty shocks. *econometrica 77*(3), 623–685.

Bloom, N. (2014). Fluctuations in uncertainty. *Journal of Economic Perspectives 28*(2), 153–176.

Burriel, P. and A. Galesi (2018). Uncovering the heterogeneous effects of ECB unconventional monetary policies across euro area countries. *European Economic Review 101*, 210–229.

Chow, G. C. and A. Lin (1971). Best linear unbiased interpolation, distribution, and extrapolation of time series by related series. *Review of Economics and Statistics 53*(4), 372–375.

Christiano, L. J., M. Eichenbaum, and C. L. Evans (1999). Monetary policy shocks: What have we learned and to what end? In M. Woodford and J. Taylor (Eds.), *Handbook of Macroeconomics*, Volume 1, pp. 65–148. Elsevier, Amsterdam.

Dees, S., F. d. Mauro, M. H. Pesaran, and L. V. Smith (2007). Exploring the international linkages of the euro area: a global VAR analysis. *Journal of Applied Econometrics 22*(1), 1–38.

Dickey, D. A. and W. A. Fuller (1979). Distribution of the estimators for autoregressive time series with a unit root. *Journal of the American Statistical Association 74*(366a), 427–431.

Fernández-Villaverde, J., J. F. Rubio-Ramírez, T. J. Sargent, and M. W. Watson (2007). ABCs (and Ds) of understanding VARs. *American Economic Review 97*(3), 1021–1026.

Gali, J. (1999). Technology, employment, and the business cycle: do technology shocks explain aggregate fluctuations? *American Economic Review 89*(1), 249–271.

Gertler, M. and P. Karadi (2015). Monetary policy surprises, credit costs, and economic activity. *American Economic Journal: Macroeconomics 7*(1), 44–76.

Ghysels, E. (2016). Macroeconomics and the reality of mixed frequency data. *Journal of Econometrics 193*(2), 294–314.

Ghysels, E., P. Santa-Clara, and R. Valkanov (2004). The midas touch: Mixed data sampling regression models. Working Paper.

Ghysels, E., A. Sinko, and R. Valkanov (2007). Midas regressions: Further results and new directions. *Econometric Reviews 26*(1), 53–90.

Giacomini, R. (2013). The relationship between DSGE and VAR models. In *VAR Models in Macroeconomics–New Developments and Applications: Essays in Honor of Christopher A. Sims*, Volume 32, pp. 1–25. Emerald Group, Bingley, UK.

Gilchrist, S., J. W. Sim, and E. Zakrajšek (2014). Uncertainty, financial frictions, and investment dynamics. NBER Working Paper No. 20038.

Hollo, D., M. Kremer, and M. Lo Duca (2012). CISS–a composite indicator of systemic stress in the financial system. ECB Working Paper, No. 1426.

Hubrich, K. and R. J. Tetlow (2015). Financial stress and economic dynamics: The transmission of crises. *Journal of Monetary Economics 70*, 100–115.

Jarociński, M. and P. Karadi (2020). Deconstructing monetary policy surprises–the role of information shocks. *American Economic Journal: Macroeconomics 12*(2), 1–43.

Jurado, K., S. C. Ludvigson, and S. Ng (2015). Measuring uncertainty. *American Economic Review 105*(3), 1177–1216.

Koop, G., M. H. Pesaran, and S. M. Potter (1996). Impulse response analysis in nonlinear multivariate models. *Journal of Econometrics 74*(1), 119–147.

Kremer, M. (2016). Macroeconomic effects of financial stress and the role of monetary policy: a VAR analysis for the euro area. *International Economics and Economic Policy 13*(1), 105–138.

Kuttner, K. N. (2001). Monetary policy surprises and interest rates: Evidence from the fed funds futures market. *Journal of Monetary Economics 47*(3), 523–544.

Lane, P. R. (2012). The european sovereign debt crisis. *Journal of Economic Perspectives 26*(3), 49–68.

Leduc, S. and Z. Liu (2016). Uncertainty shocks are aggregate demand shocks. *Journal of Monetary Economics 82*, 20–35.

Litterman, R. B. (1986). Forecasting with bayesian vector autoregressions—five years of experience. *Journal of Business & Economic Statistics 4*(1), 25–38.

Ludvigson, S. C., S. Ma, and S. Ng (2021). Uncertainty and business cycles: exogenous impulse or endogenous response? *American Economic Journal: Macroeconomics 13*(4), 369–410.

Lütkepohl, H. (2005). *New introduction to multiple time series analysis*. Springer Science & Business Media.

Mertens, K. and M. O. Ravn (2013). The dynamic effects of personal and corporate income tax changes in the United States. *American Economic Review 103*(4), 1212–47.

Nakamura, E. and J. Steinsson (2018). High-frequency identification of monetary non-neutrality: the information effect. *The Quarterly Journal of Economics 133*(3), 1283–1330.

Pesaran, H. H. and Y. Shin (1998). Generalized impulse response analysis in linear multivariate models. *Economics letters 58*(1), 17–29.

Pesaran, M. H., T. Schuermann, and S. M. Weiner (2004). Modeling regional interdependencies using a global error-correcting macroeconometric model. *Journal of Business & Economic Statistics 22*(2), 129–162.

Plagborg-Møller, M. and C. K. Wolf (2021). Local projections and vars estimate the same impulse responses. *Econometrica 89*(2), 955–980.

Rostagno, M., C. Altavilla, G. Carboni, W. Lemke, R. Motto, A. S. Guilhem, and J. Yiangou (2019). A tale of two decades: the ECB's monetary policy at 20.

Sims, C. A. (1972). Money, income, and causality. *American Economic Review 62*(4), 540–552.

Sims, C. A. (1980a). Comparison of interwar and postwar business cycles: Monetarism reconsidered. *American Economic Review 48*(1), 1–48.

Sims, C. A. (1980b). Macroeconomics and reality. *Econometrica 48*(1), 1–48.

Stock, J. H. and M. W. Watson (2012). Disentangling the channels of the 2007–2009 recession. *Brookings Papers on Economic Activity 2012*(1), 81–135.

Uhlig, H. (2005). What are the effects of monetary policy on output? results from an agnostic identification procedure. *Journal of Monetary Economics 52*(2), 381–419.

Supplementary Material to:

“Multiple Shock Impulse Response Functions”

A Derivations linear VAR

Derivation of the VMA of Equation (7) of the VAR Process

The VMA representation of the linear VAR(1) model is

$$\begin{aligned}
\boldsymbol{y}_t &= \boldsymbol{b} + \boldsymbol{B}\boldsymbol{y}_{t-1} + \boldsymbol{u}_t \\
&= \boldsymbol{b} + \boldsymbol{B}(\boldsymbol{b} + \boldsymbol{B}\boldsymbol{y}_{t-2} + \boldsymbol{u}_{t-1}) + \boldsymbol{u}_t \\
&= (\boldsymbol{I}_n + \boldsymbol{B})\boldsymbol{b} + \boldsymbol{B}^2\boldsymbol{y}_{t-2} + \boldsymbol{B}\boldsymbol{u}_{t-1} + \boldsymbol{u}_t \\
&= ... \\
&= (\boldsymbol{I}_n + \boldsymbol{B} + ... + \boldsymbol{B}^{j-1})\boldsymbol{b} + \boldsymbol{B}^j\boldsymbol{y}_{t-j} + \sum_{i=0}^{j-1}\boldsymbol{B}^i\boldsymbol{u}_{t-i},
\end{aligned}$$

by recursively substituting the VAR equation. Under Assumption 2, it holds that the sequence $\boldsymbol{B}^i$ is absolutely square summable and therefore the infinite sum of $\sum_{i=0}^{j-1}\boldsymbol{B}^i\boldsymbol{u}_{t-i}$ exists in mean square. As $j \longrightarrow \infty$, it holds that $\boldsymbol{B}^j \to \mathbf{O}$ and $(\boldsymbol{I}_n + \boldsymbol{B} + ... + \boldsymbol{B}^{j-1})\boldsymbol{b} \longrightarrow (\boldsymbol{I}_n - \boldsymbol{B})^{-1}\boldsymbol{b}$ (geometric series). Thus, when $j \longrightarrow \infty$

$$\boldsymbol{y}_t = (\boldsymbol{I}_n - \boldsymbol{B})^{-1}\boldsymbol{b} + \sum_{j=0}^{\infty}\boldsymbol{B}^j\boldsymbol{u}_{t-j}.$$

Derivation of the Impulse Response Functions

The traditional impulse response functions for a linear vector autoregression can be derived from taking the expectations of the shifted VMA representation of Equation (7) and the structural relation $\boldsymbol{\varepsilon}_t = \boldsymbol{C}\boldsymbol{u}_t$. The VMA for $\boldsymbol{y}_{t+h}$ denotes

$$\begin{aligned}
\boldsymbol{y}_{t+h} &= \boldsymbol{\mu} + \sum_{j=0}^{\infty}\boldsymbol{B}^j\boldsymbol{C}\boldsymbol{\varepsilon}_{t+h-j} \\
&= \boldsymbol{\mu} + \boldsymbol{C}\boldsymbol{\varepsilon}_{t+h} + \boldsymbol{B}\boldsymbol{C}\boldsymbol{\varepsilon}_{t+h-1} + \boldsymbol{B}^2\boldsymbol{C}\boldsymbol{\varepsilon}_{t+h-2} + ... + \boldsymbol{B}^h\boldsymbol{C}\boldsymbol{\varepsilon}_t + \boldsymbol{B}^{h+1}\boldsymbol{C}\boldsymbol{\varepsilon}_{t-1} + ...
\end{aligned}$$

Inserting the expression in both conditional expectations, this results in the perturbed path

$$\begin{aligned}
&\mathbb{E}[\boldsymbol{y}_{t+h} \mid \varepsilon_{s,t} = \delta_s, \varepsilon_{j,t} = 0\,\forall j \neq s, \boldsymbol{\varepsilon}_{t+1} = ... = \boldsymbol{\varepsilon}_{t+h} = \mathbf{0}, \boldsymbol{\omega}_t] \\
&\quad = \boldsymbol{\mu} + \mathbb{E}[\boldsymbol{C}\boldsymbol{\varepsilon}_t \mid \varepsilon_{s,t} = \delta_s, \varepsilon_{j,t} = 0\,\forall j \neq s, \boldsymbol{\varepsilon}_{t+1} = ... = \boldsymbol{\varepsilon}_{t+h} = \mathbf{0}, \boldsymbol{\omega}_t] + \boldsymbol{B}^{h+1}\boldsymbol{C}\boldsymbol{\varepsilon}_{t-1} + ... \\
&\quad = \boldsymbol{\mu} + \boldsymbol{C}\boldsymbol{e}_s\delta_s + \boldsymbol{B}^{h+1}\boldsymbol{C}\boldsymbol{\varepsilon}_{t-1} + ...
\end{aligned}$$

and the benchmark

$$\begin{aligned}
&\mathbb{E}[\boldsymbol{y}_{t+h} \mid \boldsymbol{\varepsilon}_t = \boldsymbol{\varepsilon}_{t+1} = ... = \boldsymbol{\varepsilon}_{t+h} = \boldsymbol{0}, \boldsymbol{\omega}_t] \\
&\qquad = \boldsymbol{\mu} + \mathbb{E}[\boldsymbol{C}\boldsymbol{\varepsilon}_t \mid \boldsymbol{\varepsilon}_t = \boldsymbol{\varepsilon}_{t+1} = ... = \boldsymbol{\varepsilon}_{t+h} = \boldsymbol{0}, \boldsymbol{\omega}_t] + \boldsymbol{B}^{h+1}\boldsymbol{C}\boldsymbol{\varepsilon}_{t-1} + ... \\
&\qquad = \boldsymbol{\mu} + \boldsymbol{B}^{h+1}\boldsymbol{C}\boldsymbol{\varepsilon}_{t-1} + ...
\end{aligned}$$

Thus, the difference is defined as $\boldsymbol{\Psi}^t(h, \boldsymbol{\varepsilon}_t = \delta_s, \boldsymbol{\omega}_{t-1}) = \boldsymbol{C}\boldsymbol{e}_s\delta_s$, where $\boldsymbol{e}_s$ denotes the selection vector.

In order to derive the generalized impulse response functions for a linear VAR(1) model, we split the infinite sum of the VMA as

$$\boldsymbol{y}_{t+h} = \boldsymbol{\mu} + \boldsymbol{u}_{t+h} + \boldsymbol{B}\boldsymbol{u}_{t+h-1} + ... + \boldsymbol{B}^h\boldsymbol{u}_t + \sum_{j=1}^{\infty} \boldsymbol{B}^{h+j}\boldsymbol{u}_{t-j}. \tag{A.1}$$

Next to that, as we assume normality of the residuals, we use the properties of the conditional expectations of the multivariate normal distribution in order to obtain the following expression for the expectations

$$\mathbb{E}[\boldsymbol{y}_{t+h} \mid u_{s,t} = \delta_s, \mathcal{I}_{t-1}] = \boldsymbol{\mu} + \boldsymbol{B}^h\boldsymbol{\Sigma}\boldsymbol{e}_s(\sigma_{ss})^{-1}\delta_s + \sum_{j=1}^{\infty} \boldsymbol{B}^{h+j}\boldsymbol{u}_{t-j}, \tag{A.2}$$

and

$$\mathbb{E}[\boldsymbol{y}_{t+h} \mid \mathcal{I}_{t-1}] = \boldsymbol{\mu} + \sum_{j=1}^{\infty} \boldsymbol{B}^{h+j}\boldsymbol{u}_{t-j}. \tag{A.3}$$

Again, $\boldsymbol{e}_s$ denotes the selection vector and σ_{ss} denotes the variance of shock s, i.e., the (s,s)-th entry of the covariance matrix $\boldsymbol{\Sigma}$.

For the multiple shock impulse response functions, the first conditional expectation is then

$$\begin{aligned}
\mathbb{E}[\boldsymbol{y}_{t+h} \mid \boldsymbol{u}_{\mathcal{S},t} = \boldsymbol{\delta}_{\mathcal{S}}, \mathcal{I}_{t-1}] &= \boldsymbol{\mu} + \boldsymbol{B}^h\mathbb{E}[\boldsymbol{u}_t \mid \boldsymbol{u}_{\mathcal{S},t} = \boldsymbol{\delta}_{\mathcal{S}}, \mathcal{I}_{t-1}] + \sum_{j=1}^{\infty} \boldsymbol{B}^{h+j}\boldsymbol{u}_{t-j} \\
&= \boldsymbol{\mu} + \boldsymbol{B}^h\boldsymbol{\Sigma}\boldsymbol{P}(\boldsymbol{P}'\boldsymbol{\Sigma}\boldsymbol{P})^{-1}\boldsymbol{\delta}_{\mathcal{S}} + \sum_{j=1}^{\infty} \boldsymbol{B}^{h+j}\boldsymbol{u}_{t-j},
\end{aligned} \tag{A.4}$$

where $\boldsymbol{P}$ denotes an $n \times m$ permutation matrix, containing m selection vectors where the selection indices correspond to the indices $\mathcal{S}$ of interest. The multiple shock impulse response functions are then defined as the difference between Equation (A.4) and the benchmark given by Equation (A.3).

B Application Global Vector Autoregression

Derivation of the Global Vector Autoregression (GVAR) Model

Let $\boldsymbol{y}_t$ denote a $k \times 1$ vector containing all stacked domestic variables, where $k = \sum_{i=1}^{N} k_i$, such that $\boldsymbol{y}_t = \left[\boldsymbol{y}'_{1,t}, ..., \boldsymbol{y}'_{N,t}\right]'$. We rewrite each domestic model of Equation (21) for country $i = 1, ..., N$ in terms of $\boldsymbol{y}_t$ as

$$\underbrace{\left[\boldsymbol{I}_{k_i} \quad -\boldsymbol{\Lambda}_{i,0}\right] \boldsymbol{W}_i}_{\boldsymbol{G}_{i,0}} \boldsymbol{y}_t = \boldsymbol{c}_i + \sum_{\ell=1}^{p_i} \underbrace{\left[\boldsymbol{C}_{i,\ell} \quad \boldsymbol{\Lambda}_{i,\ell}\right] \boldsymbol{W}_i}_{\boldsymbol{G}_{i,j}} \boldsymbol{y}_{t-\ell} + \sum_{\ell=0}^{q_i} \boldsymbol{\Gamma}_{i,\ell} \boldsymbol{x}_{t-\ell} + \boldsymbol{\eta}_{i,t}, \tag{A.5}$$

by splitting the sum of the country-specific exogenous variables $\boldsymbol{y}^*_{i,t}$ into a contemporaneous part and historical parts, and using Equation (22). The $(k_i + k_i^*) \times k$ country-specific weight matrix $\boldsymbol{W}_i$ contains the elements $w_{i,j}$. The first k_i rows of $\boldsymbol{W}_i$ correspond to the domestic variables itself, and the remaining k_i^* rows correspond to the selected weighted foreign variables. We stack the N domestic VAR models of Equation (A.5) as

$$\begin{bmatrix} \boldsymbol{G}_{1,0} \\ \boldsymbol{G}_{2,0} \\ \vdots \\ \boldsymbol{G}_{N,0} \end{bmatrix} \begin{bmatrix} \boldsymbol{y}_{1,t} \\ \boldsymbol{y}_{2,t} \\ \vdots \\ \boldsymbol{y}_{N,t} \end{bmatrix} = \begin{bmatrix} \boldsymbol{c}_1 \\ \boldsymbol{c}_2 \\ \vdots \\ \boldsymbol{c}_N \end{bmatrix} + \sum_{\ell=1}^{\max(p,q)} \begin{bmatrix} \boldsymbol{G}_{1,\ell} \\ \boldsymbol{G}_{2,\ell} \\ \vdots \\ \boldsymbol{G}_{N,\ell} \end{bmatrix} \begin{bmatrix} \boldsymbol{y}_{1,t-\ell} \\ \boldsymbol{y}_{2,t-\ell} \\ \vdots \\ \boldsymbol{y}_{N,t-\ell} \end{bmatrix} + \sum_{\ell=0}^{q} \begin{bmatrix} \boldsymbol{\Gamma}_{1,\ell} \\ \boldsymbol{\Gamma}_{2,\ell} \\ \vdots \\ \boldsymbol{\Gamma}_{N,\ell} \end{bmatrix} \boldsymbol{x}_{t-\ell} + \begin{bmatrix} \boldsymbol{\eta}_{1,t} \\ \boldsymbol{\eta}_{2,t} \\ \vdots \\ \boldsymbol{\eta}_{N,t} \end{bmatrix}, \tag{A.6}$$

or as

$$\boldsymbol{G}_0 \boldsymbol{y}_t = \boldsymbol{c} + \sum_{\ell=1}^{\max(p,q)} \boldsymbol{G}_\ell \boldsymbol{y}_{t-\ell} + \sum_{\ell=0}^{q} \boldsymbol{\Gamma}_\ell \boldsymbol{x}_{t-\ell} + \boldsymbol{\eta}_t, \tag{A.7}$$

with $p = \max_i(p_i)$ and $q = \max_i(q_i)$. We rearrange Equation (A.7) as

$$-\boldsymbol{\Gamma}_0 \boldsymbol{x}_t + \boldsymbol{G}_0 \boldsymbol{y}_t = \boldsymbol{c} + \sum_{\ell=1}^{q} \boldsymbol{\Gamma}_\ell \boldsymbol{x}_{t-\ell} + \sum_{\ell=1}^{\max(p,q)} \boldsymbol{G}_\ell \boldsymbol{y}_{t-\ell} + \boldsymbol{\eta}_t. \tag{A.8}$$

We then rewrite the common variable equation Equation (23) as

$$\boldsymbol{x}_t - \boldsymbol{\Phi}_0 \widetilde{\boldsymbol{W}} \boldsymbol{y}_t = \boldsymbol{c}_x + \sum_{\ell=1}^{p_x} \boldsymbol{\Theta}_\ell \boldsymbol{x}_{t-\ell} + \sum_{\ell=1}^{q_x} \boldsymbol{\Phi}_\ell \widetilde{\boldsymbol{W}} \boldsymbol{y}_{t-\ell} + \boldsymbol{\eta}_{x,t}. \tag{A.9}$$

Both Equation (A.8) and Equation (A.9) have a similar structure. We then stack the common variable model on the N domestic models and obtain

$$\underbrace{\begin{bmatrix} \boldsymbol{I} & -\boldsymbol{\Phi}_0 \widetilde{\boldsymbol{W}} \\ -\boldsymbol{\Gamma}_0 & \boldsymbol{G}_0 \end{bmatrix}}_{\boldsymbol{H}_0} \begin{bmatrix} \boldsymbol{x}_t \\ \boldsymbol{y}_t \end{bmatrix} = \begin{bmatrix} \boldsymbol{c}_x \\ \boldsymbol{c} \end{bmatrix} + \sum_{\ell=1}^{\max(p,q,q_x)} \underbrace{\begin{bmatrix} \boldsymbol{\Theta}_\ell & \boldsymbol{\Phi}_\ell \widetilde{\boldsymbol{W}} \\ \boldsymbol{\Gamma}_\ell & \boldsymbol{G}_\ell \end{bmatrix}}_{\boldsymbol{H}_\ell} \begin{bmatrix} \boldsymbol{x}_{t-\ell} \\ \boldsymbol{y}_{t-\ell} \end{bmatrix} + \begin{bmatrix} \boldsymbol{\eta}_{x,t} \\ \boldsymbol{\eta}_t \end{bmatrix}, \tag{A.10}$$

or

$$\boldsymbol{H}_0 \boldsymbol{z}_t = \boldsymbol{h}_0 + \sum_{\ell=1}^{\max(p,q,q_x)} \boldsymbol{H}_\ell \boldsymbol{z}_{t-\ell} + \boldsymbol{\varepsilon}_t, \tag{A.11}$$

where $\boldsymbol{z}_t = [\boldsymbol{x}_t', \boldsymbol{y}_t']'$, $\boldsymbol{h}_0 = [\boldsymbol{c}_x', \boldsymbol{c}']'$ and $\boldsymbol{\varepsilon}_t = [\boldsymbol{\eta}_{x,t}', \boldsymbol{\eta}_t']'$. In this structural specification, $\boldsymbol{H}_0$ captures the contemporaneous relations between the variables. Provided that $\boldsymbol{H}_0$ is invertible, i.e., the structural model Equation (A.11) is assumed to be stable, we obtain the reduced-form VAR given by

$$\boldsymbol{z}_t = \boldsymbol{k}_0 + \sum_{\ell=1}^{\max(p,q,q_x)} \boldsymbol{K}_\ell \boldsymbol{z}_{t-\ell} + \boldsymbol{u}_t, \tag{A.12}$$

where $\boldsymbol{k}_0 = \boldsymbol{H}_0^{-1}\boldsymbol{h}_0$, $\boldsymbol{K}_\ell = \boldsymbol{H}_0^{-1}\boldsymbol{H}_\ell$ for all lags, and the residuals $\boldsymbol{u}_t = \boldsymbol{H}_0^{-1}\boldsymbol{\varepsilon}_t$ with $\mathbb{E}[\boldsymbol{u}_t\boldsymbol{u}_t'] = \boldsymbol{H}_0^{-1}\boldsymbol{\Sigma}_e(\boldsymbol{H}_0^{-1})' = \boldsymbol{\Sigma}_u$. Note that in light of Equation (8), $\boldsymbol{C} = \boldsymbol{H}_0^{-1}$.

Bayesian Estimation Procedure

In this section we discuss the Bayesian estimation method we use to obtain the parameters of the reduced-form VAR of the domestic models and common variable models, (21) and (23). Following Lütkepohl (2005), let the model below denote a general matrix notation for a VARX(p,q) models, with n endogenous variables and n_{ex} exogenous variables. That is,

$$\boldsymbol{Y} = \boldsymbol{X}\boldsymbol{B} + \boldsymbol{E}, \tag{A.13}$$

where $\boldsymbol{Y}$ is a $(T-p)\times n$ matrix containing the n endogenous variables. The right-hand side $(T-p)\times(np+n_{ex}(q+1)+1)$ matrix $\boldsymbol{X}$ containing all lags of the VAR, including exogenous variables, and a constant, and $\boldsymbol{B}$ denotes the corresponding coefficient matrix. The residuals $\boldsymbol{E}$ have variance-covariance matrix $\boldsymbol{\Sigma}$.

The prior on $\boldsymbol{B}$ and $\boldsymbol{\Sigma}$ is an independent normal-inverted Wishart prior, such that $p(\boldsymbol{B},\boldsymbol{\Sigma}) = p(\boldsymbol{B})p(\boldsymbol{\Sigma})$, with

$$\boldsymbol{\Sigma} \sim \mathcal{IW}(\boldsymbol{S}_0, v_0) \propto |\boldsymbol{\Sigma}|^{-v_0/2} \exp\Big(-\frac{1}{2}\mathrm{tr}(\boldsymbol{S}_0)\boldsymbol{\Sigma}^{-1}\Big), \tag{A.14}$$

and

$$\mathrm{vec}(\boldsymbol{B}) \sim \mathcal{N}(\mathrm{vec}(\boldsymbol{B}_0), \boldsymbol{V}_0) \propto \exp\Big(-\frac{1}{2}\mathrm{vec}(\boldsymbol{B}-\boldsymbol{B}_0)'\boldsymbol{V}_0^{-1}\mathrm{vec}(\boldsymbol{B}-\boldsymbol{B}_0)\Big), \tag{A.15}$$

where vec is the vectorization operator, $\mathcal{IW}$ is the inverted-Wishart distribution and $\mathcal{N}$ is the normal distribution.

The prior parameter $v_0 = N+2$ and S_0 is a diagonal matrix with σ_i^2 on its diagonal, where σ_i denotes the standard error in a $AR(p)$ model of variable i. In $\boldsymbol{B}_0$ we set the coefficient the diagonal element corresponding to the first lag to one if the corresponding variable is non-stationary according to the ADF test (Dickey and Fuller, 1979), and zero otherwise. All remaining entries are zero. The matrix $\boldsymbol{V}_0$ is a diagonal matrix, where each element corresponds to the implied standard deviation of lag ℓ of variable j in equation i, which is equal to $\lambda_1\sigma_i/\sigma_j\ell^{-\lambda_2}$. We set $\lambda_1 = 0.2, \lambda_2 = 1$ as in Litterman (1986) and Jarociński and Karadi (2020).

The posterior distribution of $\boldsymbol{\Sigma}$ is

$$\boldsymbol{\Sigma}|\boldsymbol{B},\boldsymbol{X} \sim \mathcal{IW}(\overline{\boldsymbol{S}},\overline{v}), \text{ with } \overline{\boldsymbol{S}} = \boldsymbol{S}_0 + \boldsymbol{E}'\boldsymbol{E} \text{ and } \overline{v} = v_0 + T, \tag{A.16}$$

where the latter two equations are updating equations. The posterior distribution of $\boldsymbol{B}$ is

$$\text{vec}(\boldsymbol{B})|\boldsymbol{\Sigma},\boldsymbol{X} \sim \mathcal{N}(\text{vec}(\overline{\boldsymbol{B}}),\overline{\boldsymbol{V}}), \tag{A.17}$$

$$\overline{\boldsymbol{V}} = (\boldsymbol{V}_0^{-1} + \boldsymbol{\Sigma}^{-1} \otimes \boldsymbol{X}'\boldsymbol{X})^{-1}, \text{ and } \text{vec}(\overline{\boldsymbol{B}}) = \overline{\boldsymbol{V}}\big(\boldsymbol{V}_0^{-1}\text{vec}(\boldsymbol{B}_0) + (\boldsymbol{\Sigma}^{-1} \otimes \boldsymbol{X}')\text{vec}(\boldsymbol{Y})\big).$$

We use Gibbs sampling to compute the posterior distribution. To compute the complete posterior distribution, we sample in an iterative manner from (A.16) and (A.17) until the sampler converges.

GVAR Model Statistics

Below are model diagnostics reported. The left figure shows that there is indeed weak cross-sectional dependence in the idiosyncratic shocks—over 70% of the residuals have a contemporaneous correlation of lower than 0.2. The right figure shows that the majority of the residuals are weakly autocorrelated. The trade-based weights are indeed relatively small. We further assume that the trade-based weights and GDP weights are constant over time. This is a reasonable assumption, as the relative trade relations and relative GDPs between the four countries do not change too much in our sample. All in all, this GVAR specification seem to capture the complex dynamics between countries well, and adequately satisfy the GVAR assumptions.

Figure A.1: Model statistics GVAR

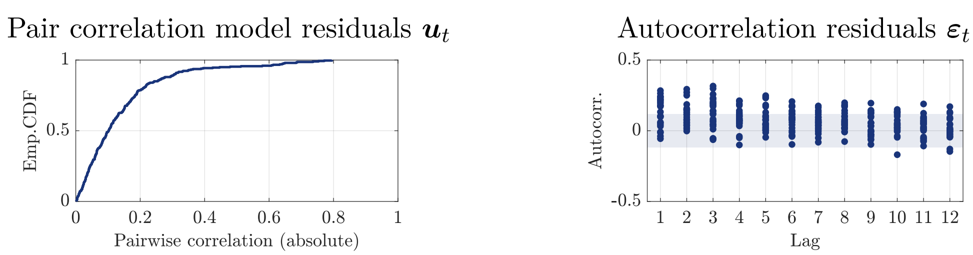

		Import				Eigenvalues	
		FRA	GER	ITA	SPN	Max.	Min.
Export	FRA	-	0.46	0.31	0.40	0.9965	0.0144
	GER	0.54	-	0.54	0.40		
	ITA	0.25	0.36	-	0.20		
	SPN	0.21	0.17	0.15	-		
	$\widetilde{\boldsymbol{w}}$ (GDP)	0.28	0.37	0.21	0.14		

Note: Autocorrelation and pairwise correlation is reported for the residuals in the two figures. The table reports the trade-based weights between the countries in 2014, the GDP weights between the countries, and the maximum and minimum eigenvalues of the median model.